Nanoscale

Accepted Manuscript

This article can be cited before page numbers have been issued, to do this please use: A. Singh, T. Ye and N. J. Wittenberg, *Nanoscale*, 2026, DOI: 10.1039/D5NR05126F.

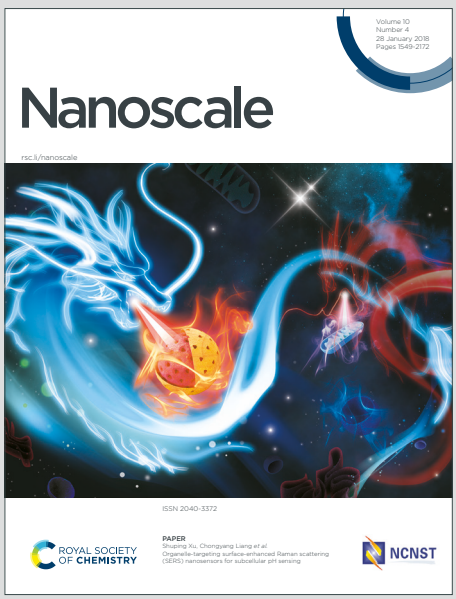

ROYAL SOCIETY OF CHEMISTRY

rsc.li/nanoscale

View Article Online
DOI: 10.1039/D5NR05126F

Advances in Multivariate Analysis of Extracellular Vesicles Using Visible Light-Based Analytical Methods

Aarshi N. Singh[1], Tiffany T. Ye[1], Nathan J. Wittenberg[1]*

[1]Department of Chemistry, Lehigh University, Bethlehem, PA, 18015, U.S.A.
*Corresponding author: Nathan J. Wittenberg
Email: njw@lehigh.edu

Abstract:

Extracellular vesicles have emerged as promising candidates for diagnostic and therapeutic applications, however their inherent heterogeneity presents significant challenges for their characterization and implementation. A number of visible light-based analytical techniques have emerged to examine the physicochemical properties of extracellular vesicles in ensembles and as individual entities. We discuss how these methods can be utilized to analyze multiple parameters simultaneously, providing a more comprehensive understanding of the distribution of extracellular vesicle properties. These techniques offer insights into the interconnected forms of heterogeneity, including the interplay between size, biomolecular composition, and interactions. This review surveys the current landscape of multivariate heterogeneity analysis, highlighting its potential for advancing extracellular vesicle-based therapies.

View Article Online
DOI: 10.1039/D5NR05126F

Introduction:

An interesting feature of both prokaryotic and eukaryotic cells is their ability to secrete smaller portions of their membranes to create nanoscale (10's-100's nm-diameter) membrane-bound vesicles. These vesicles possess several biochemical components, such as lipids, nucleic acids, and proteins, that in some respects resemble their parent cell, which makes them attractive as potential therapeutic or diagnostic agents[1,2] (**Fig. 1A**). These secreted vesicles are broadly categorized as extracellular vesicles (EVs), however depending on their origin, they can be further classified as microvesicles (also referred as ectosomes), exosomes, or apoptotic bodies[3–5]. The precise mechanism of microvesicle production remains unclear. However, studies have shown that the translocation of phosphatidylserine, facilitated by floppase, to the outer leaflet of the membrane, coupled with actin-myosin cytoskeleton contraction, facilitates membrane pinching, leading the formation of microvesicles that range from 100-1000 nm in diameter (**Fig. 1B**)[6,7]. In contrast to microvesicles, exosomes are smaller (30-100 nm diameter) and are secreted through a more well-defined subcellular mechanism. Exosomes are produced through the endosomal sorting complex required for transport (ESCRT) pathway, which plays a pivotal role in the formation of early endosomes (**Fig. 1B**). This pathway mediates the sorting of cargo into intraluminal vesicles within the multivesicular body (MVB), which are subsequently released as exosomes upon fusion of the MVB with the plasma membrane[6,7]. Lastly, apoptotic bodies are membrane-bound vesicles that span a wide size range (50-5000 nm). These EVs are formed during apoptosis, containing fragmented cellular components such as organelles, nuclear material, and cytoplasmic content[8]. The minimal information for studies of extracellular vesicles (MISEV 2023) guidelines recommend using the term "extracellular vesicles" for vesicle classification unless their exact mechanism of origin can be determined[9]. Therefore, this review will primarily use the term "EVs" for eukaryotic vesicles, except where the original authors have specified otherwise. In addition to addressing issues of nomenclature, the MISEV 2023 guidelines are also concerned with issues such as EV isolation methods and purity assessment, and we will highlight these aspects when discussing specific examples from the literature.

Similar to eukaryotes, prokaryotes have also been reported to form vesicles that are involved in intercellular communication and pathogenesis[10]. Gram-negative bacteria possess a dual-membrane structure and are capable of shedding their outer membrane to form nanometer-sized vesicles (50-250 nm diameter) known as outer membrane vesicles (OMVs) (**Figure 1B)**. In addition to genetic material, lipids, and proteins found in EVs and exosomes, some OMVs also contain toxins[11–13]. More recently, it has been reported that a small population of vesicles of bacterial origin, known as inner outer membrane vesicles (IOMVs), contain both the inner and outer membranes of gram-

View Article Online
DOI: 10.1039/D5NR05126F

negative bacteria and carry cytoplasmic DNA[14,15]. Similarly, gram-positive bacteria have been observed to produce vesicles derived from their cytoplasmic membrane[10,16,17].

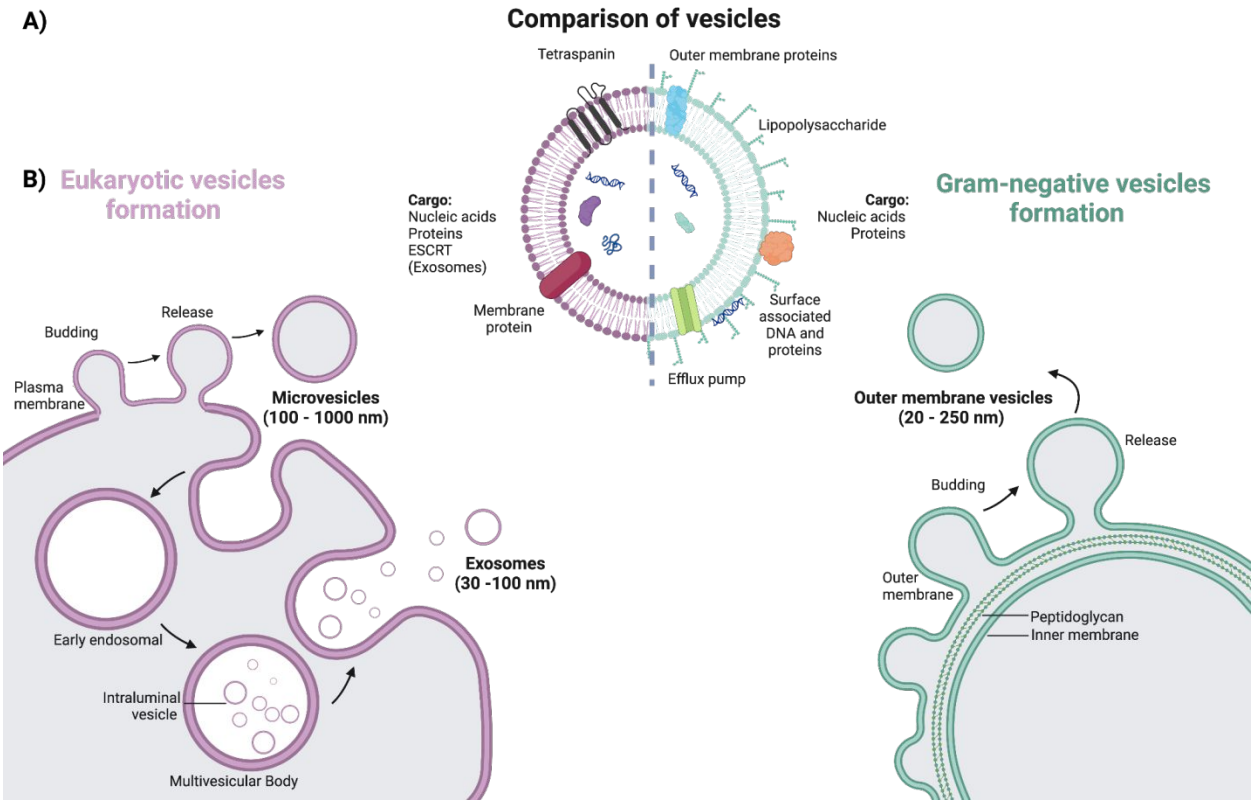

Fig. 1: Schematic diagram of extracellular vesicle composition and formation: (A) Structure comparison of vesicles: Purple half vesicle (left) represent a eukaryotic vesicle components, while the green half vesicle (right) represents a gram-negative bacteria vesicle components. **(B)** The purple cell (left) represents a eukaryotic cell capable of producing two distinct types of vesicles through different pathways. Microvesicles bud directly from the plasma membrane, whereas exosomes are formed through a defined pathway. In this pathway, the plasma membrane first buds inward to form early endosomes, which then undergo further inward budding to generate intraluminal vesicles, resulting in the formation of multivesicular bodies. These multivesicular bodies subsequently fuse with the plasma membrane to release exosomes. The green cell represents (right) a gram-negative bacteria, where smaller fragments of outer membrane are secreted to form the OMVs.

In addition to mammalian and bacterial cells, plant cells also secrete EVs, which have been shown to play critical roles in plant growth, tissue repair, and defending against pathogens[18–20]. Structurally, plant derived EV's (PDEV) are similar to mammalian and bacterial cell vesicles. containing lipids, proteins, and nucleic acids and have shown potential to be used a cancer therapeutics[21,22]. Recent advances in the EV field have further identified exercise-induced extracellular vesicles and vesicles released from

View Article Online
DOI: 10.1039/D5NR05126F

surgical tissues, highlighting the expanding complexity and biological diversity of this field[23–25].

EVs and OMVs have shown promise in medical applications. EVs have great potential as diagnostic tools because studies have shown that EVs often carry specific biomarkers, which can serve as reliable agents for disease detection and monitoring[26,27]. Earlier reports have shown that EVs derived from stem cells possess regenerative potential, serving as a critical mediator of tissue repair and regeneration[28,29]. Furthermore, exosomes play a crucial role in neurological intracellular communication, and their ability to cross the blood-brain barrier while preserving the integrity of their biological cargo makes them an ideal candidate for neurochemical biomarker detection[30,31]. OMVs, due to their composition that can include lipopolysacharides and toxins from the parent bacteria, have the ability to trigger an immune response making them possible vaccine candidates[32–34]. Despite the appeal, EV use in the pharmaceutical industry has been limited due to a variety of factors, including their heterogeneity. Regardless of being isolated from the same culture, EVs exhibit several heterogeneous features, such as size and cargo differences[35–37]. Deciphering EV heterogeneity is essential for their use in therapeutic applications, since heterogeneities lead to a difference in function[12,38]. The inherent heterogeneity, coupled with nanoscale sizes make analytical examination of EVs challenging. Fortunately, several optical methods **(Table 1)** have been developed to identify and analyze EV heterogeneity. Using methods that allow for the detection of several heterogeneous parameters (size, biomolecular content, etc.) simultaneously is essential as it allows for a broader and more comprehensive understanding of these nanoscale particles. Previous research and review articles have provided valuable insights into the current landscape of optical-based analytical methods[39,40]. Building on these foundational studies, we offer a new perspective by further examining and contextualizing recent advances of commonly used multivariate analysis methods that have contributed to the understanding of the physical and biochemical multiple properties of EVs using optical based methods. While there are several optical based analytical methods that can be used to analyze EVs, in this review, we primarily focus on visible light based methods due to their ease, minimal sample prep requirement, and growing presence in the EV analysis.

Technique Family	Optical Category	General Characteristics	Detection capabilities	Sample Preparation
Fluorescence/ Visible light microscopy/	Visible light	Spatial resolution depends on technique, single EV measurements	single EV and molecule detection; multiple markers	Minimal prep; immobilized or suspended samples

View Article Online
DOI: 10.1039/D5NR05126F

Flow cytometry	Visible light	Single EV measurements	Multiple markers; rare event detection challenging	Debris and non-EV particles must be removed
Vibrational spectroscopy/ Raman/ FT-IR	Visible light Infrared light	Ensemble measurement, chemically sensitive/selective	Varies, can be enhanced (e.g. SERS, SEIRA)	Bulk solution or immobilized samples; minimal prep
Interferometric Scattering Microscopy (iSCAT)	Visible light interferometry	Single EV measurement; can be combined with fluorescence	Single particle detection; EV sizing	Clean surface, immobilized particles often required.

Table 1: Comparison of different light based analytical methods and their detection limit, detection sensitivity and sample preparation[41–45].

Optical microscopy methods

Microscopy is a powerful tool for analyzing EVs, since it facilitates simultaneous visualization and multiparametric analysis. There are several different microscopic methods that can be used to analyze vesicles. Light microscopy has several advantages for EV analysis such as minimal sample preparation, real time observation, and ability to incorporate multiple fluorescent dyes. However, light microscopy also has disadvantages that limit its potential, such as diffraction limit challenges. Due to the diffraction limit of light, particles smaller than approximately 200 nm appear as diffraction limited spots when visualized with traditional fluorescence microscopy methods. While the diffraction limit prohibits substructural analysis, there are many examples of fluorescence microscopy being applied to EV analysis[46,47]. Of course, super-resolution optical microscopy methods can offer improved resolution, and in fact, some commercial super-resolution systems are marketed with EV analysis in mind. Furthermore, light microscopy may be affected by background noise originating from EV aggregation or co-isolated protein aggregates, which can generate signals that are difficult to distinguish from those of individual vesicles.

Beyond optical microscopy, other microscopic techniques can be used to analyze EVs. The assorted variants of electron microscopy, such as scanning electron microscopy (SEM), transmission electron microscopy (TEM), and cryo-TEM have advantages in examining the nanoscale properties of EVs, however, their extensive sample preparation steps can lead to artifacts. Furthermore, this family of methods provides static snapshots which limits their ability to monitor dynamic processes. In addition to EM, scanning probe microscopies, for example atomic force microscopy (AFM), can be used to circumvent

View Article Online
DOI: 10.1039/D5NR05126F

diffraction-limited resolution. A major advantage of AFM is that it can probe mechanical properties of EVs, and it can be combined with fluorescence microscopy for multiparametric analysis[48]. While EM and AFM can achieve better spatial resolution than optical microscopies, in this section we generally limit our discussion to advances fluorescence microscopy for multiparametric EV analysis. As previously mentioned, bacterial and eukaryotic vesicles often exhibit multiple heterogeneities, such as variations in size or the presence of specific proteins, which may or may not be interconnected. For example, larger vesicles might contain proteins absent in smaller vesicles, or vesicle size could influence their interactions with host cells[38]. Microscopic methods are essential for this analysis, as they not only allow visualization of the sample but also enable protein tagging through antibody labeling, which enables simultaneous detection of heterogeneity amongst multiple proteins[49].

Leveraging advanced microscopic techniques for multi-protein labeling via multiple fluorescently labeled antibodies, Nikoloff et al. developed a promising new method that allows for detection of up to four extracellular vesicle proteins[50]. In this work, the authors developed a new microfluidic device designed to capture single cells and the EVs that are being secreted by them. Since the parent cells were contained in the same device as the analyzed EVs, the purity of EVs was not assessed by orthogonal methods. The EVs are immobilized using antibodies specific to the tetraspanin protein CD63 and further analyzed using four-color total internal reflection fluorescence (TIRF) microscopy to understand the abundance of multiple surface proteins simultaneously **(Fig. 2A-C)**. By examining the co-expression of these proteins, the authors observed an intriguing pattern: HER2 showed a negative correlation with CD81, meaning that EVs with high HER2 expression tended to have comparatively lower levels of CD81 **(Fig. 2D)**.

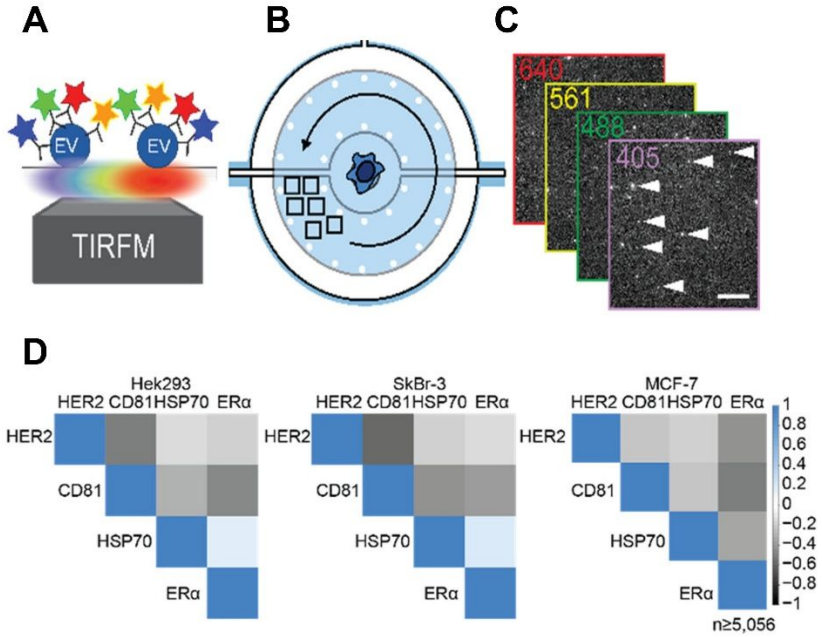

View Article Online
DOI: 10.1039/D5NR05126F

Fig. 2. Multiparametric analysis of individual EVs with TIRF microscopy. (A-B) Using fluorescently conjugated mAbs and four-color TIRF microscopy, immobilized EVs were imaged in the direct neighborhood of the cells. which are prevented from cross-contamination with EVs from other cells. (C) Multicolor TIRFM images of secreted and immobilized EVs. (D) Correlation analysis of analyzed markers on detected EV populations. Correlation analysis, showing a weak positive association of HSP70 to integral ERα. Overexpressed membrane proteins, like CD81, HER2, and ERα show negative correlation with most other proteins due to its abundant integration into membranes. Protein overexpression disguises protein colocalization in EV membranes. This figure has been adapted from reference 50 with permission from the American Chemical Society, copyright 2023.

Integration of fluorescence microscopy with AFM can yield information that is invisible to either method alone. For example, Cavallaro et al. combined AFM and fluorescence microscopy to conduct single EV measurements for simultaneous determination of vesicle size and stiffness along with relative protein abundances via protein-specific antibodies[48]. In this study, they obtained EVs from three different cell lines: embryonic kidney, cord blood mesenchymal stromal, and leukemia cell lines, and tried to determine the abundance of different tetraspanins (membrane-associated EV proteins) in addition to the size and stiffness of the EVs. Their method revealed that CD81 was the most abundant tetraspanin in the EVs derived from the embryonic kidney cell line, while CD63 was more abundant in EVs from mesenchymal stromal cells. Additionally, it was reported that the EVs from the embryonic kidney cell line were more likely to express all three tetraspanins (CD9, CD63, and CD81) compared to EVs from other cell types. Additionally, it was reported that the EVs expressing all three of the tetraspanins were smaller in size, however, they displayed a considerable size variation. Furthermore, it was found that mesenchymal and leukemia cell EVs containing both CD9 and CD63 were smaller in size than those containing only CD81. These findings underscore the importance of analyzing multiple markers simultaneously to capture a more nuanced understanding of EV characteristics. While the two above examples employed tetraspanins as EV markers, it is important to note that not all EVs possess similar distributions of tetraspanins, with some EVs lacking one or many. For this reason, the use of a single tetraspanin for capture of EVs, for example, can be risky since the absence (or heterogeneous distribution) of that tetraspanin on the EVs would lead to incomplete or biased capture of the EVs from a population, thus biasing measurements and conclusions derived from them.

Recently, Singh et al. steered multivariate analysis in the in the direction of OMVs, where they demonstrated the ability to detect protein toxin (leukotoxin A, LtxA) sorting based on vesicle size[12]. In this method, OMVs are first biotinylated which allows for the immobilization on streptavidin passivated glass. This immobilization scheme is beneficial for capturing all OMVs, eliminating discrepancies related to heterogeneously expressed native proteins present on their surface. In this study, OMVs are labeled with a

View Article Online
DOI: 10.1039/D5NR05126F

membrane-specific fluorescent dye, enabling the calculation of their integrated fluorescence intensity, which is then used to determine their size distribution. After size determination, the immobilized OMVs are exposed to LtxA-specific antibodies, enabling the detection of the toxin on their surface. A secondary antibody is then used for colocalization of the OMV and the toxin, confirming the presence of the LtxA. OMVs are further categorized into LtxA-positive and LtxA-negative groups, allowing for the identification of size-dependent LtxA sorting. This approach revealed that larger OMVs were significantly more likely to contain the LtxA compared to smaller OMVs, emphasizing the crucial role of vesicle size in bacterial toxin sorting.

While understanding protein-size and protein-protein colocalization is important, EVs are also enriched with other intravesicular components, such as nucleic acids, which play crucial roles in their function[4]. However, despite the appeal, detecting intravesicular components can be challenging due to the requirement of lysing the EV. Given the challenges in analyzing both intravesicular and extravesicular components, Li et al. developed an innovative single-EV analysis method which enables the colocalization analysis between protein and microRNA (miRNA)[51]. In this technique, the authors used the NanOstirBar (NOB)-Enabled Single Particle Analysis (NOBEL-SPA) assay. This approach uses magnetic NOB particles conjugated with antibodies specific to a chosen tetraspanin protein, enabling efficient capture of EVs from the supernatant based on the presence of these surface proteins. Once the EVs are captured, they are lysed using detergent to expose the intravesicular miRNA, which is further crosslinked to the EV proteins or the NOB antibodies to prevent diffusion of the contents. The exposed miRNA is further analyzed using a hairpin probe, which is designed with a complementary sequence to the target miRNA and a primer region for rolling circle amplification (RCA), which forms DNA nanoflowers (DNF) labeled with fluorescent probes for detection using confocal microscopy. To identify colocalization between proteins and miRNAs, specific aptamer-containing probes were designed to detect individual proteins, each paired with a corresponding miRNA probe. The protein probes generate a DNF labeled with Alexa 647 for protein detection, while the miRNA probes are labeled with Alexa 488. This innovative method enables colocalization experiments with different biological components, highlighting the significance of a multivariate analysis platform for studying complex molecular interactions.

Microarray-based methods

For several years, microarray-based methods have gained significant attention for their applications in biochemical assays and medical settings. In a microarray-based assay, simultaneous analysis of thousands of EVs is possible. In this application, a capture probe, such as a protein or nucleic acid, is printed onto a substrate, typically a microscopic slide, to selectively bind the target structure. This targeted binding enables

View Article Online
DOI: 10.1039/D5NR05126F

further analysis of surface proteins or other molecular features[52]. In the context of EV microarray assays, often times protein microarray technology is employed, using specific proteins as capture probes to bind EV surface proteins selectively[53]. This targeted capture allows for detailed multivariate analysis of EV surface markers, with results typically read out using a microarray scanner that detects fluorescent or chemiluminescent signals from the EVs. Microarray-based methods offer several advantages for EV analysis, including ease of implementation, high-throughput capability, multiplex biomarker detection, and the requirement for relatively small sample volumes. However, these approaches also present several limitations, most notably capture bias. Because EV detection relies on antibody-mediated capture, only vesicles expressing the targeted surface proteins will be detected. As the understanding of EV heterogeneity continues to evolve, it is increasingly evident that not all EV populations share the same surface markers, which may lead to incomplete representation of the vesicle population[12,38]. Furthermore, these assays provide limited information regarding EV size, as vesicles can be captured and detected on the array but accurate size characterization remains challenging. In this section, we review the recent advances in EV multivariate analysis using micro-based assay.

In one example, Martel et al. developed an innovative microarray method of high-throughput, multiplexed analysis of EV inner and outer proteins (EVPio), that enables detection of proteins present on the outer surface of the EVs, as well as identification of intra-vesicular EV proteins[54]. Prior to analysis, EVs were purified by size exclusion chromatography, assayed for total protein content, and their concentration was determined by tunable resistance pulse sensing. In this method, ten distinct antibody microarray spots were printed onto a 2D polyaldehyde slide using an inkjet printer, and EVs from two different colorectal cancer cells were subsequently immobilized on the surface **(Fig. 3A-B)**. To detect colocalized inner and outer proteins, the EVs were fixed and permeabilized using surfactants which facilitates the detection of both of the proteins. Given the low abundance of inner and outer membrane proteins, the authors employed a novel approach to enhance detection. They added a DNA barcode to each antibody, and after the antibodies bound to their target proteins, a complementary fluorescent DNA strand was introduced for signal readout. This method amplified the signal, improving the detection sensitivity for low-abundance proteins. As a proof of concept, this method was tested on EVs from two genetically modified colorectal cell lines, which revealed a generally similar inner-outer protein composition. It would be interesting to extend this method to EVs from different cancer types, for example breast vs colon, and compare results about the outer-inner protein heterogeneity.

View Article Online
DOI: 10.1039/D5NR05126F

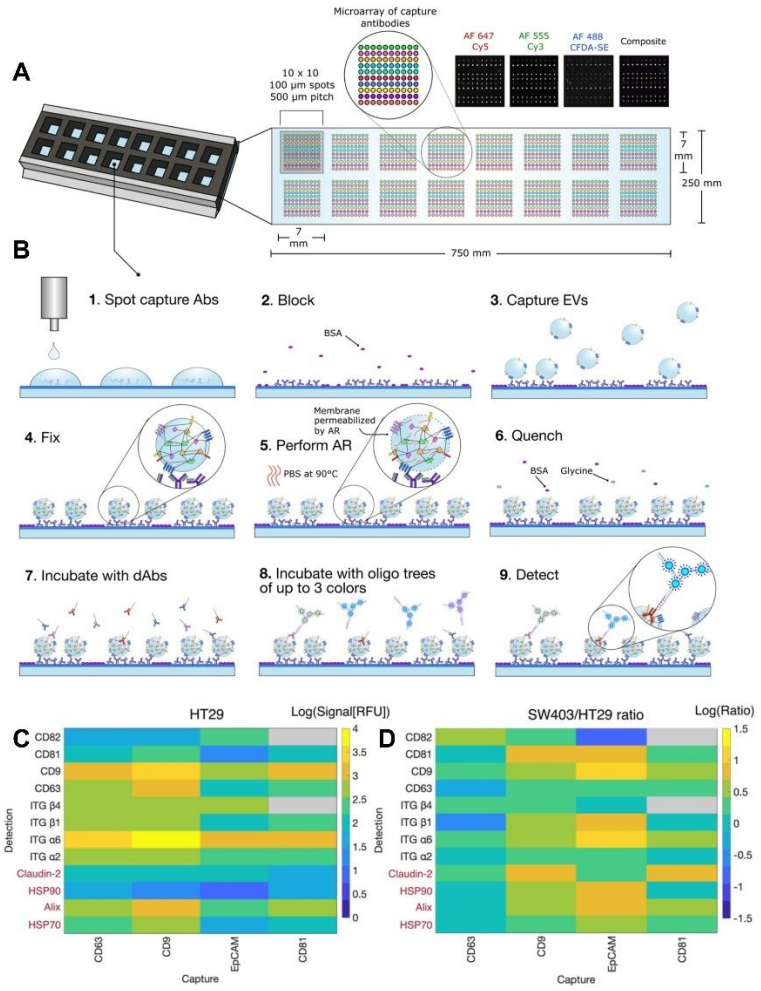

Fig. 3. EVPio: combinatorial profiling of extracellular vesicle inner and outer proteins. (A) The EVPio assay is performed on a well gasket-covered glass slide that has been inkjet printed with 16 10 × 10 subarrays of antibodies, where each row targets a different EV surface protein. (B) EVPio workflow: (1) capture antibodies are inkjet printed on a functionalized slide (PolyAn 2D-Aldehyde), (2) the slide is washed and unoccupied sites are blocked, (3) the sample is incubated on the antibody spots and the EVs are captured based on their surface protein markers, (4) bound EVs are fixed on the slide, (5) the slide is AR treated, (6) quenched to get rid of the remaining reactive groups, (7) the slide is washed and incubated with up to three different oligo barcode-conjugated primary detection antibodies, (8) the slide is washed and incubated with complementary fluorescently labeled oligonucleotide constructs (up to three colors), and (9) immobilized immunolabeled EVs are detected using a confocal microarray scanner. Microspots, antibodies, oligonucleotides, and EVs are not to scale. This figure has been adapted from reference 54 with permission from the American Chemical Society, copyright 2022.

Clegg et al. also developed a multiparametric microarray designed to profile multiple surface proteins simultaneously[55]. In their method, the protein antibodies are printed on an epoxy silane coated slide to capture EVs that express those proteins on their surface. The authors printed three specific antibodies, CD9, CD81, and CD63 as microarray spots to target proteins commonly associated with EVs. Additionally, they

View Article Online
DOI: 10.1039/D5NR05126F

prepared a cocktail combining these antibodies along with heat shock protein 90 (HSP90) and flotillin to enable multi-protein detection and analyze the diverse protein composition of EVs. In this study, samples from six healthy blood donors were analyzed to investigate the multivariate variations in protein abundance.

A similar approach was used by Cawley et al. to analyze bacterial vesicles from pathogenic bacteria *A. Actinomycetemcomitans*[56]. Given the smaller size of OMVs, instead of microprinting the array, the authors employed liftoff nanocontact printing[57]. In this method, they printed two different antibodies, anti-LtxA (leukotoxin-specific) and anti-OmpA (outer membrane protein A), to assess whether OMVs would bind to them and hence capture them on the surface. The multivariate analysis in this assay hinges on the capturing agent used, as it enables differentiation between OMVs containing the toxin and those that do not highlight the potential of arrayed assay in the realm of bacterial infection diagnostics.

Surface plasmon resonance methods

Surface plasmon resonance (SPR) is an optical technique that relies on the change in the refractive index near the surface of a sensor upon adsorption of mass[58]. Because SPR measures minute changes in refractive index, its major advantage is that it does not require any extraneous labels for the analytes of interest. The instrumental configuration of SPR can vary from the traditional Kretschmann configuration[59], where a uniform gold film and a prism are required, to nanoplasmonic approaches where surface plasmons confined to nanoscale features are exploited for label-free detection[60]. These advantages and configuration versatility makes SPR an excellent tool for analyzing EVs and their interactions with antibodies or other binding agents, without the need for labels. SPR is also commonly used to analyze a variety of biomolecular interactions, providing insights into binding kinetics and affinity[61]. Similar to microarray-based methods, SPR also has limitations: it suffers from capture bias, provides no direct information on EV morphology, and can be affected by non-specific binding that reduces measurement accuracy. In recent years, SPR has become a widely used method for EV analysis, where specific antibodies are coated onto the surface to capture vesicles based on their protein expression profiles[62–64]. For an extensive review on SPR and other plasmonic sensors for EV analysis, the reader is directed to the article by Im and coworkers[65].

In one example of SPR for EV analysis, Hsu et al. developed an innovative method combining SPR and surface plasmon-enhanced fluorescence spectroscopy within a single platform, enabling the simultaneous detection of proteins and miRNA that exosomes carry[66]. In this approach, exosomes are initially immobilized on the SPR chip through antibodies targeting the specific protein of interest. Subsequently, a molecular beacon probe, specific for a miRNA, was added to the chamber and the increase in fluorescence intensity upon hybridization was observed. In this study, the authors

View Article Online
DOI: 10.1039/D5NR05126F

investigated the relative expression ratio between surface proteins and miRNA present in exosomes derived from lung and breast cancer cells. For the exosomes derived from breast cancer cells, the presence of the membrane protein ANXA8, known for its elevated expression, and miR-342, downregulated compared to control cells, were investigated. Additionally, for the lung cancer cell derived exosomes, membrane proteins EGFR and LG3BP, along with miR-21 and miR-210 were analyzed. EGFR and LG3BP have been reported for tumor growth and metastasis, and miR-21 and miR-210 regulate signaling pathways making them critical biomarkers for lung cancer diagnosis. This platform allows for simultaneous detection of several cancer biomarkers and enables an enhanced sensitivity to differentiate cancer cells from healthy cells, potentially leading to precise diagnosis through complementary expression ratios of multiple biomarkers.

In 2020, Yang et al. reported an SPR-based biosensing platform coupled with surface plasmonic resonance microscopy (SPRM) for multiparametric analysis[67]. This method enables the simultaneous detection of EV size distribution, concentration, and molecular interaction affinity. The latter was determined by assessing the binding of EVs to surface-bound CD63 antibodies, which facilitated their capture and subsequent characterization. Since the intensity of the SPRM signal correlates with the size of the vesicles, the authors first immobilized the EVs on the surface and measured the signal intensity to obtain the size distribution. Additionally, since binding on the SPR chip relies on diffusion and particle concentration, the authors established a linear relationship between EV count and sensor surface binding, enabling determination of EV concentration from the sample. This method enhances the ability to use SPR to understand the different physical properties of vesicles.

Advanced nanofabrication techniques have enabled advances in the development of nanoplasmonic sensors capable of SPR-based multiparametric analysis of EVs. These sensors offer the ability to densely pack discrete sensing zones in a small footprint for integration with microfluidic channels to enable multiplex assays. An example of nanoplasmonic SPR implementation for profiling of EVs is the nPLEX assay[68], which is based extraordinary optical transmission through a periodic array of sub-wavelength diameter holes in a gold film. With this type of transmission-mode SPR, the magnitude of spectral shift of light transmitted through the nanohole array is associated with exosomes binding to the sensor. Alternatively, the change in transmission intensity at a fixed wavelength can be used for signal readout. In the nPLEX assay, exosomes are bound on the surface of the gold nanohole film by various antibodies that probe for the presence of exosome-related surface markers, such as CD63, CD24, and EpCAM. The magnitude of normalized signal (spectral shift or intensity change) is proportional to the amount of exosomes bound to the chip, and thus the density of the specific exosome marker on the exosome surface. Using this approach, Im and coworkers demonstrated the ability to identify biomarker profiles for exosomes derived from ovarian cancer cells. They were

View Article Online
DOI: 10.1039/D5NR05126F

also able to detect cancer exosomes from patient-derived body fluids and use the assay to monitor cancer response or progression during chemotherapeutic treatment.

While the nPLEX assay demonstrated impressive results, the primary markers of interest were transmembrane proteins found on the surface of the EVs. To advance the technology, the same group developed a nanohole SPR-based approach to analyze the intravesicular proteins of EVs that were isolated by ultracentrifugation[69]. In this assay, termed intravesicular nanoplasmonic system (iNPS), EV lysate is exposed to gold nanohole arrays that are functionalized with antibodies to capture intravesicular or transmembrane proteins associated with EVs. Upon binding to the surface immobilized antibodies, the proteins of interest are subsequently bound by gold nanoparticles (AuNPs) decorated with antibodies **(Fig. 4A-B)**, which serve to greatly amplify signals up to 9-fold due to enhanced electromagnetic field intensity near the nanohole rims **(Fig. 4C-D)**. The authors found a limit of detection of 10^4 EVs. To validate the assay, the authors examined signals arising from the binding of intact EVs and EV lysates to antibody-functionalized nanohole arrays, along with EV lysates with AuNP amplification **(Fig. 4E)**. It was found that AuNP amplification was necessary to detect markers from EV lysates, including the intravesicular marker ATK1. The new assay was further validated by examining the correlation between protein levels measured by traditional ELISA assays and iNPS. The authors found good correlation between the two different measurement techniques **(Fig. 4F**). Next, seven different EV-associated markers were probed, including both transmembrane and intravesicular proteins in EVs as well as in their parent cells. The obtained signals, and therefore the expression levels, of these markers were in strong correlation with cellular expression levels **(Fig.4G)**.

View Article Online
DOI: 10.1039/D5NR05126F

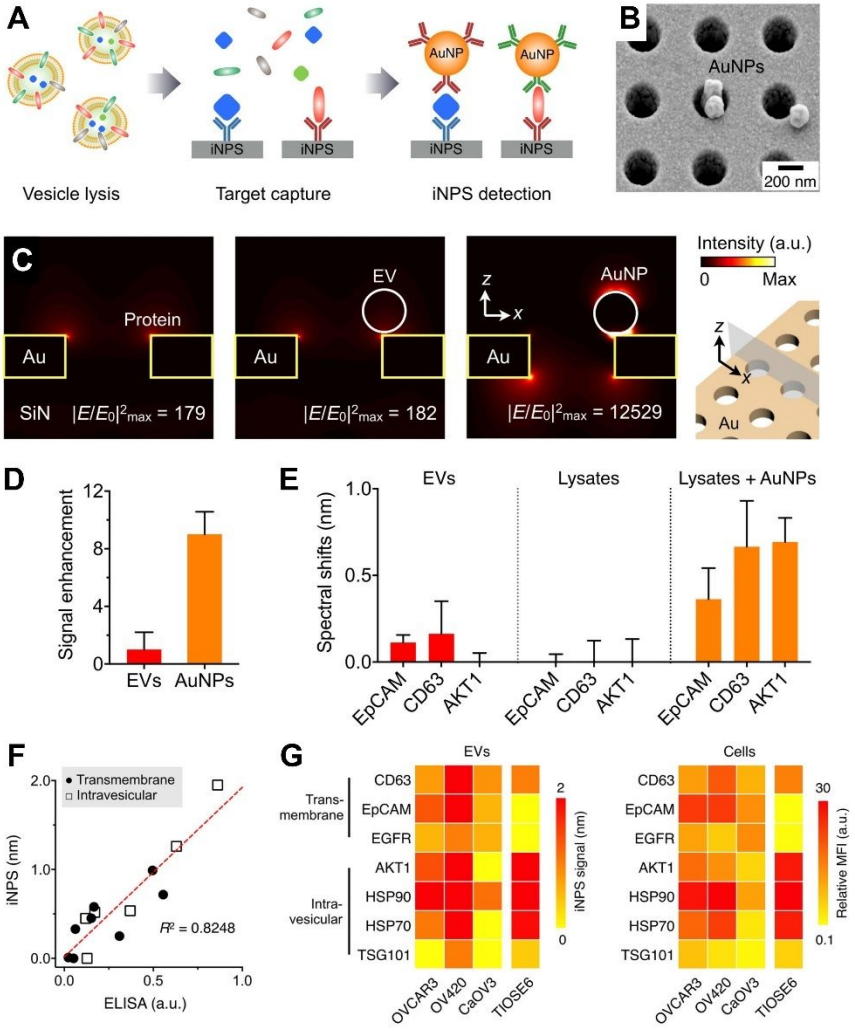

Fig. 4. Overview of the iNPS assay. (A) EVs are lysed to release molecular cargos. Each target is captured on the iNPS chip via affinity ligands, and further labeled with Au nanoparticles (AuNPs). (B) Scanning electron micrograph showing AuNPs after iNPS assay steps. (C) FDTD electromagnetic simulation. AuNP on the iNPS surface concentrates electrical fields. Compared to a protein binding (left) or a whole EV binding (middle), the field intensity enhanced up to 70-fold with AuNP (right). (D) Measured signal enhancement. Compared to EV binding, the spectral shift was about 9-fold higher when the same concentration of AuNPs (100 nm) bound to the iNPS chip. (E) Validation of iNPS assay. AuNPs enables both membrane protein (EpCAM, CD63) and intravesicular protein (AKT1) detection with enhanced spectral shifts. The error bars represent the standard deviation of signals. (F) iNPS and ELISA were used to detect intravesicular (HSP90, HSP70, TSG101) and transmembrane proteins (CD63, EpCAM, EGFR). The results from both methods showed a good correlation (R^2 = 0.8248). For iNPS assays, we used 108 EVs per marker and measured spectral shifts. Note that ELISA required 200-fold larger amount of samples than iNPS. (G) Protein profiling of ovarian cells and their secreting EVs. Transmembrane (CD63, EpCAM, EGFR) and intravesicular (AKT1, HSP90, HSP70, TSG101) protein levels were measured. Cellular protein expression of three ovarian cancer cell lines (OV420, CaOV3, and OVCAR3) and one benign cell lines (TIOSE6) were measured by flow cytometry. EVs secreted from those cells were analyzed by iNPS. Overall, EV protein expression patterns were correlated

View Article Online
DOI: 10.1039/D5NR05126F

with cellular expression patterns. This figure has been adapted from reference 69 with permission from the American Chemical Society, copyright 2018.

Light scattering methods

When a particle interacts with incident light, the light can either be absorbed or induce polarization within the particle. This polarization oscillates in sync with the incident light, causing some of the light to scatter which can be studied to understand physical properties about the size, molecular weight, etc. In light scattering methods, two primary scattering mechanisms are commonly studied, Rayleigh scattering and Mie scattering. Depending on the particle size and the wavelength of the incident light, either of the scattering is observed. Rayleigh scattering is observed when the particle size is 10 times smaller than the wavelength of the incident light. The observed scattering is elastic, where the frequency of the light remains unchanged, producing consistent scattering in all directions. In contrast, Mie scattering arises when the particle size is less than one-tenth of the wavelength. The scattering intensity varies with each angle, indicating its dependence on the angle of measurement[70–72]. Light scattering provides label-free, average size and polydispersity measurements of an EV population in a relatively fast and easy fashion. Furthermore, light scattering methods can be added to the additional analytical techniques such as flow cytometry and multi-angle light scattering. However, it also has several disadvantageous such as its bias towards larger sized particles in a heterogenous size population and requires high sample concentration[73,74]. Additionally, flow cytometry and Raman spectroscopy, detailed in the following sections, use light scattering to analyze the vesicles. Here we discuss some of the common light scattering methods that are used to analyze vesicles.

Dynamic light scattering (DLS), nano tracking analysis (NTA), static light scattering (SLS), and multi-angle light scattering (MALS) are essential techniques commonly used to characterize vesicles[75–79]. When incident light, typically a laser in these methods, interacts with vesicles, a portion of the light is scattered. This scattered light provides insights into the diffusion behavior of the particles, enabling the determination of their size, shape, and dynamic properties. DLS measures the Brownian motion of particles by analyzing time dependent fluctuations in the intensity of scattered light. Brownian motion, diffusional movement of the particles in a fluid, is size dependent; meaning the larger particles scatter more light than the smaller particles. The intensity fluctuations are correlated together to obtain an autocorrelation function which allows for the calculation of vesicles translational diffusion coefficient. The diffusion coefficient can then be used to obtain vesicle size using the Stokes-Einstein equation[80,81]. DLS measures vesicles as a population, however recent advancements in NTA allows for single vesicle analysis. NTA employs a similar principle where the Brownian motion of vesicles is measured and the mean square displacement is reported of individual vesicles[82,83].

View Article Online
DOI: 10.1039/D5NR05126F

In contrast to DLS, SLS measures the average scattering intensity of particles dispersed in a solution. By evaluating how light interacts with these particles, the technique enables the determination of their molecular mass and radius of gyration, which is described as the root mean square distance of the scattering mass distribution from the center of mass of the particle. This provides insights into the particle's size and shape[84]. SLS provides valuable information, however it is better suited for larger particles. DLS is more commonly used for vesicle analysis due to its higher sensitivity to smaller particles. Though, a combination of SLS and DLS has been reported to analyze vesicle size and shape[85,86]. A variation to SLS is MALS. In this method, additional detectors are present which allow for the determination of the scattering light at multiple angles[87].

In an interesting example where a combination of orthogonal separation, scattering, and fluorescence analytical techniques enabled multivariable analysis, Normak et al. were able to characterize the concentration of particles, average diameter of the particles, protein to particle ratio, presence of EV surface markers and lipids, EV shape, and sample purity. They did this by employing an instrument that integrated liquid chromatography coupled with MALS and fluorescence detection[88]. The chromatographic separation step allowed analysis of both crude and purified samples. With this setup, the sample underwent liquid chromatography first to isolate the analyzed vesicles. Next, the MALS detector is used to analyze the size and concentration of particles in the sample. Finally, the sample is put through the FLD component to measure the intrinsic fluorescence of proteins and the fluorescence signal of specific markers[88]. Impressively, with this strategy they were able to fully characterize samples that contained as few as 10^7 particles.

To demonstrate their methods capabilities, Normak et al. analyzed EVs derived from HEK293-F cells. Total number of particles determined by MALS analysis were in general agreement with results from nanoparticle tracking analysis (NTA), with the MALS method yielding a slightly larger number of particles than NTA. The authors reasoned that the reported discrepancy may be due to low separation resolution and the obscuration of smaller particles by larger particles[90]. The average diameter of the size distribution of particles measured with MALS method was consistent with both NTA and DLS analysis, with the result being 148 nm across all techniques. Additionally, the SEC followed by MALS analysis can be further coupled with FLD to measure the total protein amount of EVs. These additional integrated techniques enable enhanced multiparametric results from the method.

NTA is inherently a multiparametric technique because it provides information about the size, concentration, and vesicle count. However, it can have disadvantages as well since NTA cannot differentiate between vesicles versus other small contaminants. Therefore, it is critical to optimize the sample preparation and protocol to obtain high

View Article Online
DOI: 10.1039/D5NR05126F

quality data. Comfort et al. provide a detailed protocol for EV preparation and method parameters to obtain vesicle size and concentration from a NTA measurement[89].

Flow cytometery methods

Flow cytometry is a powerful tool that is commonly used for multivariate characterization of cells and EVs. In this method, particles (cells or EVs) pass through a laser beam in a single-file manner, enabling the analysis of individual vesicles. This alignment is achieved by applying a sheath fluid, typically a buffer solution, to guide the vesicles into a streamlined flow. As the particles pass through the laser, they scatter light that is measured in two directions, forward and side scattering. Forward scattering is used to detect particle size by measuring the light scattered in the same direction as the laser beam. Side scattering, captured at a 90° angle to the laser path, provides information about the internal complexity of the vesicles[90]. Additionally, labeling the particles with fluorescent tags can provide information about the abundance of specific biomarkers. Labeling the sample with a fluorescent tag offers the additional advantage of enabling its use in imaging flow cytometry. Imaging flow cytometry combines traditional flow cytometry with high-resolution imaging, allowing for the analysis of both the quantitative and morphological properties of individual cells or particles. In this technique, as the particles pass through the laser, the microscope's add-on components capture images of the particles[91]. This allows for morphological analysis of the cells in addition to the conventional flow cytometry results.

Flow cytometry is commonly used for EV analysis due to its high throughput capabilities, ability to perform multivariate analysis, and minimum sample preparation. However, it also suffers from several disadvantages such as the requirement for instrumentation modification or high sensitivity flow cytometers to accommodate EVs smaller size and weak light scattering. For instance, Arkesteijn et al. demonstrated that forward light scatter can be enhanced by using adjusted obscuration bars and pinhole, to reduce optical background noise and enable reliable detection of the nanoscale sizes particles[92]. Another commonly used technique used to analyze EV through conventional flow cytometer is to capture the EVs on a large bead, which helps with the resolution of flow cytometer[93].

Despite the challenges, low cytometry and its variations are commonly used to analyze different types of vesicles, such as EVs[94–96], exosomes[97,98], and bacterial OMVs[38,99,100]. By utilizing fluorescent labeling and multiparametric analysis, flow cytometry enables the characterization of complex vesicle populations with high sensitivity and resolution. Flow cytometry's ability to detect a wide range of parameters makes it a great method for analyzing the multiparametric characteristics of vesicles. To elucidate the function of vesicles, it is critical for the sample to be pure and accurately represent their biological components. However, many of the conventional methods for isolation often carry limitations including low purity, low yield, long duration, large sample

View Article Online
DOI: 10.1039/D5NR05126F

requirements, specialized equipment, highly trained personnel, and high costs. To address these issues, Sharma et al. introduced a novel insulator-based dielectrophoretic (iDEP) device capable of rapidly isolating nanoscale EVs from cell culture media based on their size and dielectric characteristics[101]. More specifically, the array of micropipettes within their iDEP device applies an electric field of ~10 V/cm across the lengths of the pipettes, allowing isolation of nanoparticles from small sample volumes. After purifying the EVs, the authors employed flow cytometry, both imaging and conventional, as well as next-generation miRNA sequencing to validate the purity of the vesicles derived from their system.

The authors identified heterogeneity among EVs expressing the tetraspanins CD63 and CD81. Specifically, it was reported that 55% serum, 31% plasma, 30% urine EVs contained CD63, while 22% serum, 41% plasma, 34% urine EVs contained CD81. Imaging flow cytometry showed that extracellular vesicles derived from serum had the highest expression levels of both CD63 and CD81, followed by those derived from plasma, with those from urine having the lowest levels. Furthermore, microRNA sequencing revealed mature 137 miRNA transcripts across all EV samples, revealing that iDEP device is sensitive at retaining the inherent miRNA associated with vesicles. The authors also compared the results of the iDEP-purified vesicles with those from traditional purification methods, such as differential ultracentrifugation and size exclusion chromatography, and observed similar patterns in the retained biomarkers and miRNA. This demonstrates that iDEP can effectively purify EVs.

Protein and nucleotide cargo of EVs are well studied, their lipid composition and how it contributes to EV heterogeneity is less known. While membrane order and lipid packing can be mimicked with multicomponent bilayers in synthetic liposomes created with controlled lipid composition, bulk lipid membrane studies of EVs demonstrates variation in lipid composition. This variability had not been well evaluated at the single EV level. Single-EV flow cytometry methods allow for the characterization of molecular cargos on a single vesicle basis. However, there is a limitation with flow speed due to the prevalence of the so-called swarm effect, where a group of small particles may register as a single large particle. Von et al. developed a method they coined, EV Fingerprinting, to unwind the complexity of EV populations whilst being able to achieve accurate high-throughput detection of small particles at a fast flow rate (~100,000 events/min)[102] Additionally, this group used this device in conjunction with the uptake of lipophilic environment-sensitive membrane probes di8 by the lipid bilayer to create their single-EV flow cytometry method. In this method, the authors utilized an intriguing membrane probe, di8, which provides insights into both the relative size of the EVs and their membrane order properties. Additionally, the authors analyzed EV cargo by using antibodies specific to target proteins or through intrinsic labeling of the proteins.

View Article Online
DOI: 10.1039/D5NR05126F

Using this method, the authors were able to investigate multiple parameters involved in EV biogenesis. For instance, the authors found that knockout Rab27a, a protein involved in EV biogenesis, led to a decrease in the production of membrane ordered EV, while the membrane disordered EVs were unaffected. Interestingly, a different trend was observed when CD63 where the smaller EVs were more membrane ordered, however, the larger EV had more cargo present compared to the control EVs. This underscores the importance of using multivariable analysis to assess EV heterogeneity, enabling a more comprehensive understanding of their diverse roles and functions.

Raman spectroscopy methods

Raman spectroscopy is a type of vibrational spectroscopy that exploits the inelastic scattering of photons. The Raman scattering phenomenon is extremely weak, with only a tiny fraction of scattered photons being inelastically scattered due to the small Raman cross-sections of most molecules[103]. Raman scattered photons exhibit characteristic wavenumber shifts associated with vibrational modes of different chemical functional groups. Peaks in a Raman spectrum are narrower than peaks in a fluorescence spectrum, thus reduced spectral overlap of Raman peaks makes this method ideally suited to the simultaneous detection of multiple analytes. Like infrared absorbance, Raman spectroscopy is capable of functional group identification, but unlike infrared, Raman is compatible with aqueous solutions due to water's small Raman scattering cross section. Clearly, the combination of narrow peak widths, functional group-specific signals, and water compatibility make Raman spectroscopy a powerful technique for biochemical analysis.

Despite these advantages, the inherent weakness of Raman signals can hamper its implementation. To boost Raman signals, amplification strategies are often employed, most notably surface-enhanced Raman scattering (SERS)[104]. In SERS, scattering signals from molecules that are within a few nanometers of a roughened or nanoparticle metal surface, most typically gold or silver, can be enhanced by widely ranging factors that can be as high as 10^{12} [105]. This enhancement arises from separate electromagnetic and chemical mechanisms[106,107] that are beyond the scope of this review.

The substantial increase in signals afforded by SERS has been exploited for detection and identification of a broad span of biochemical analytes, including biomarkers on the surface of EVs. In one example, Lin and coworkers used SERS for phenotyping EVs by using gold nanoparticle SERS nanotags coated with antibodies against CD63, PD-L1 or EGFR markers[108]. In this study, the EVs were isolated by centrifugation, and their morphology was determined by SEM. Each type of SERS nanotag had a single type of antibody on its surface, as well as a single type of Raman label, either mercaptobenzoic acid (MBA), 2-nitrobenzoic acid (DTNB), or 2,3,5,6-tetrafluoromercaptobenzoic acid

View Article Online
DOI: 10.1039/D5NR05126F

(TFMBA). In this assay, each type of SERS nanotag could bind a specific marker (CD63, PD-L1, or EGFR) on the EVs, and the binding would be read out by the detection of SERS signals from the label (MBA, DTNB, or TFMBA) at distinct Raman shifts. To enrich the EVs and SERS nanotags in the detection zone, magnetic beads functionalized with CD63 were also introduced. CD63 is a general EV marker and should bind EVs regardless of the phenotype. The magnetic beads were magnetically-enriched in the detection zone, probed with a laser, and the SERS spectrum was collected. A schematic of the device and operation principle of the assay is shown in **Fig. 5A,B**. With this platform, the authors assayed EVs originating from three different cell lines, NCI-H226 and A549 lung cancer cells and BEAS-2B cells derived from normal lung bronchial epithelial cells line, and detection limits as low as 4.46×10^2 EVs/mL were determined. EVs from these cells clearly display different expression levels of the CD63, PD-L1, and EGFR markers **(Fig. 5C-F)**. Using chemometric analysis, the authors were able to readily distinguish EVs based on their cellular origin **(Fig. 5G)**.

View Article Online
DOI: 10.1039/D5NR05126F

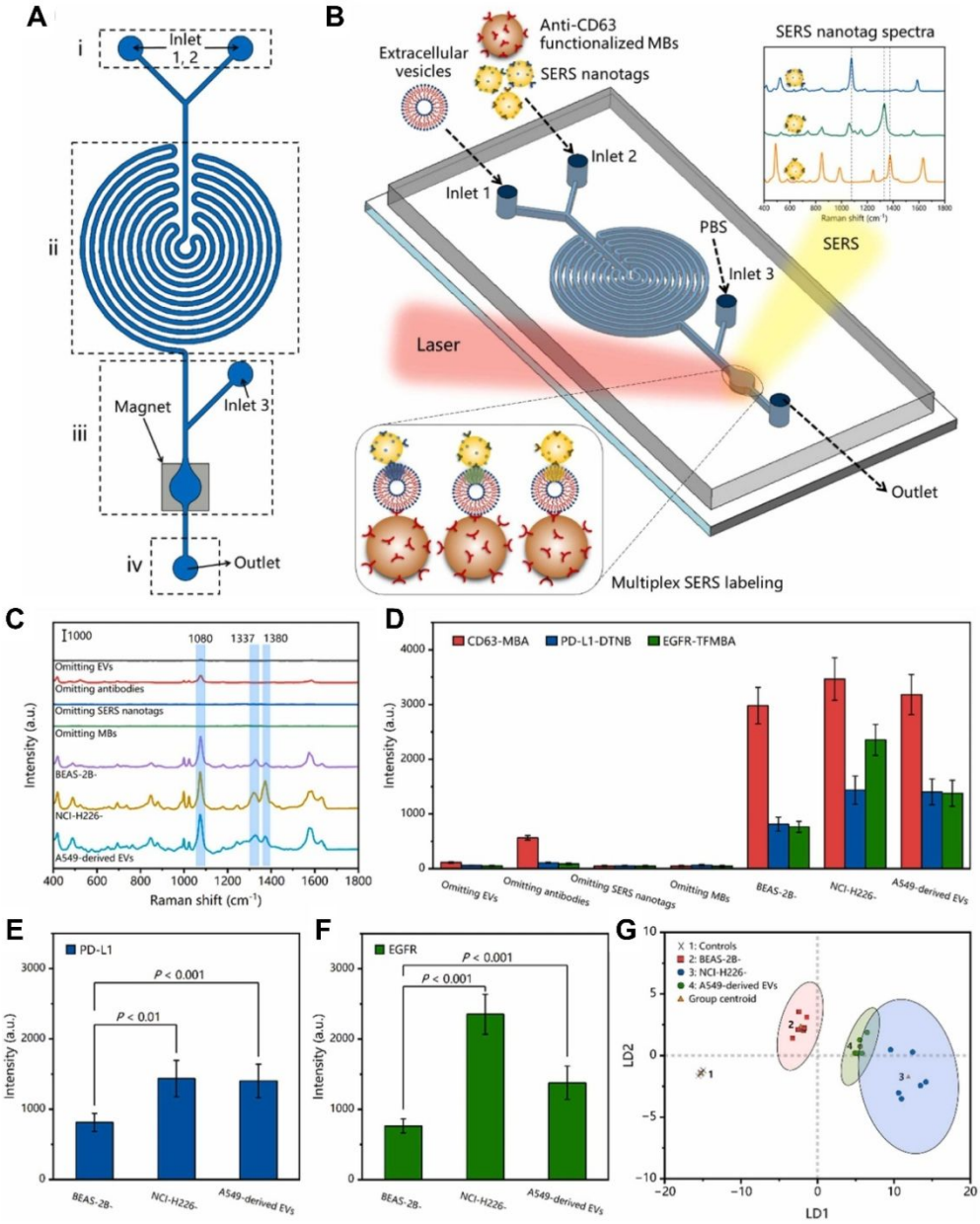

Fig. 5. SERS-based phenotyping of EVs. (A) Schematic structure of the microfluidic device with (i) sample inlet ports, (ii) a serpentine channel for mixing EVs, SERS nanotags, and magnetic beads, (iii) a zone for magnetic capture of labeled EVs, washing, and SERS detection, and (iv) a sample outlet port. (B) Operational principle of the microfluidic device showing sample introduction, EV capture with magnetic beads and labeling with SERS nanotags, and the distinct SERS spectra of the SERS nanotags possessing the different Raman labels. Phenotyping of EVs derived from lung cancer cell lines (NCI-H226 and A549) and normal lung bronchial epithelial cell line (BEAS-2B) using the on-chip SERS platform were tested for their (C) SERS spectra and (D) SERS signatures. Negative controls included omitting EVs, antibodies, SERS nanotags, or MBs. Comparison of (E) PD-L1 and (F) EGFR levels on EVs derived from three cell lines. *P* values were calculated by independent t-tests. (G) Classification of various cell line-

View Article Online
DOI: 10.1039/D5NR05126F

derived EVs via linear discriminant analysis (LDA) of their SERS signatures. The RPMI 1640 media were used as controls. The red, green, and blue circles show 95 % confidence ellipses (two-sided). Data is represented as mean ± s.d. This figure has been adapted/reproduced from reference 108 with permission from Elsevier, copyright 2023.

The use of tagged nanoparticles that give rise to well-defined SERS signatures, as is done in the previous example **(Fig. 5)**, can simplify EVs profiling. However, this approach is limited in that it is able to detect only markers that are predefined. To exploit the full richness of SERS spectra in examining the biochemical constitution of EVs, groups have analyzed the intrinsic SERS signal arising from the EVs themselves, in the absence of extrinsic tags. This presents challenges, however, because the SERS spectra tend to be quite complex with few readily identifiable spectral features that vary between EV type. To overcome these challenges, researchers often turn to machine learning approaches.

In one example, Diao and coworkers were able to discriminate exosomes from noncancerous H8 cells and cervical (HeLa) and breast (MCF-7) cancer cell lines[109]. To do this, they engineered a multilayer film of AuNPs that had a high density of SERS hotspots, then individually adsorbed exosomes from each cell type to the AuNP film. Examination of the SERS spectra for exosomes of each cell type enabled the identification of 7-9 distinct Raman bands, with many of the bands observable in all of the different exosomes. Due to the slight variation in spectra across exosome types, the authors sequentially applied principal component analysis (PCA) and linear discriminant analysis (LDA) to identify two factors that could be used to classify exosomes based on cellular origin. Next, exosomes from clinical samples were analyzed. These included exosomes from health patients, along with those from cervical and breast cancer patients. Using the algorithm developed on cell line-derived exosomes, it was possible to predict the patient origin of the exosomes with 100% accuracy for cervical and breast cancer and 80% accuracy for healthy patients. Finally, this analytical workflow was used to assess the mechanisms of doxorubicin (DOX), a chemotherapeutic agent, on MCF-7 breast cancer cells. By examining the SERS spectra of MCF-7 cell-derived exosomes at various time points after DOX treatment, it was found that DOX caused protein structure alterations that led to cell death.

Conclusion and outlook:

In conclusion, while EVs hold significant potential for diagnostic and therapeutic applications, their inherent heterogeneity remains a major challenge for their widespread use in medicine. Advances in analytical techniques, such as flow cytometry, microscopy, and optical spectroscopy now allow for more comprehensive studies of EVs by enabling simultaneous assessment of multiple parameters. Recent studies highlighted in this review demonstrate significant progress in improving the characterization and

View Article Online
DOI: 10.1039/D5NR05126F

understanding of EV properties, which is crucial for biomedical applications. We also discussed how different forms of heterogeneity, such as size variations and the interplay between proteins or protein-miRNA complexes, are interlinked. This emphasizes the importance of considering multiparametric heterogeneity rather than focusing on a single parameter. The field is evolving by enhancing common benchtop methods to improve their analytical capabilities. Recent advances have also introduced artificial intelligence (AI) into EV research. Several groups have reported AI-driven and machine learning–based approaches capable of predicting and identifying potential biomarkers present on EV surfaces from complex biological datasets for use in precision drug delivery[110–112]. These computational strategies enable the analysis of large, multidimensional datasets and can reveal molecular patterns that may be difficult to detect using conventional analytical methods. As a result, AI-assisted analysis is emerging as a powerful complementary tool for EV characterization, biomarker discovery, and improving the sensitivity and throughput of existing analytical platforms. Looking ahead, further refinement of these methods and development of new methods addressing current challenges will be critical for advancing EV-based diagnostics and therapies in clinical settings.

Acknowledgements: This work was supported by a grant from the National Institutes of Health (R15GM152918).

View Article Online
DOI: 10.1039/D5NR05126F

References:

(1) Mir, B.; Goettsch, C. Extracellular Vesicles as Delivery Vehicles of Specific Cellular Cargo. *Cells* **2020**, *9* (7), 1601. https://doi.org/10.3390/cells9071601.
(2) Jabalee, J.; Towle, R.; Garnis, C. The Role of Extracellular Vesicles in Cancer: Cargo, Function, and Therapeutic Implications. *Cells* **2018**, *7* (8), 93. https://doi.org/10.3390/cells7080093.
(3) Doyle, L.; Wang, M. Overview of Extracellular Vesicles, Their Origin, Composition, Purpose, and Methods for Exosome Isolation and Analysis. *Cells* **2019**, *8* (7), 727. https://doi.org/10.3390/cells8070727.
(4) Van Niel, G.; D'Angelo, G.; Raposo, G. Shedding Light on the Cell Biology of Extracellular Vesicles. *Nat. Rev. Mol. Cell Biol.* **2018**, *19* (4), 213–228. https://doi.org/10.1038/nrm.2017.125.
(5) Gurung, S.; Perocheau, D.; Touramanidou, L.; Baruteau, J. The Exosome Journey: From Biogenesis to Uptake and Intracellular Signalling. *Cell Commun. Signal.* **2021**, *19* (1), 47. https://doi.org/10.1186/s12964-021-00730-1.
(6) Akers, J. C.; Gonda, D.; Kim, R.; Carter, B. S.; Chen, C. C. Biogenesis of Extracellular Vesicles (EV): Exosomes, Microvesicles, Retrovirus-like Vesicles, and Apoptotic Bodies. *J. Neurooncol.* **2013**, *113* (1), 1–11. https://doi.org/10.1007/s11060-013-1084-8.
(7) Abels, E. R.; Breakefield, X. O. Introduction to Extracellular Vesicles: Biogenesis, RNA Cargo Selection, Content, Release, and Uptake. *Cell. Mol. Neurobiol.* **2016**, *36* (3), 301–312. https://doi.org/10.1007/s10571-016-0366-z.
(8) Zhou, M.; Li, Y.-J.; Tang, Y.-C.; Hao, X.-Y.; Xu, W.-J.; Xiang, D.-X.; Wu, J.-Y. Apoptotic Bodies for Advanced Drug Delivery and Therapy. *J. Controlled Release* **2022**, *351*, 394–406. https://doi.org/10.1016/j.jconrel.2022.09.045.
(9) Welsh, J. A.; Goberdhan, D. C. I.; O'Driscoll, L.; Buzas, E. I.; Blenkiron, C.; Bussolati, B.; Cai, H.; Di Vizio, D.; Driedonks, T. A. P.; Erdbrügger, U.; Falcon-Perez, J. M.; Fu, Q.; Hill, A. F.; Lenassi, M.; Lim, S. K.; Mahoney, M. G.; Mohanty, S.; Möller, A.; Nieuwland, R.; Ochiya, T.; Sahoo, S.; Torrecilhas, A. C.; Zheng, L.; Zijlstra, A.; Abuelreich, S.; Bagabas, R.; Bergese, P.; Bridges, E. M.; Brucale, M.; Burger, D.; Carney, R. P.; Cocucci, E.; Crescitelli, R.; Hanser, E.; Harris, A. L.; Haughey, N. J.; Hendrix, A.; Ivanov, A. R.; Jovanovic-Talisman, T.; Kruh-Garcia, N. A.; Ku'ulei-Lyn Faustino, V.; Kyburz, D.; Lässer, C.; Lennon, K. M.; Lötvall, J.; Maddox, A. L.; Martens-Uzunova, E. S.; Mizenko, R. R.; Newman, L. A.; Ridolfi, A.; Rohde, E.; Rojalin, T.; Rowland, A.; Saftics, A.; Sandau, U. S.; Saugstad, J. A.; Shekari, F.; Swift, S.; Ter-Ovanesyan, D.; Tosar, J. P.; Useckaite, Z.; Valle, F.; Varga, Z.; Van Der Pol, E.; Van Herwijnen, M. J. C.; Wauben, M. H. M.; Wehman, A. M.; Williams, S.; Zendrini, A.; Zimmerman, A. J.; MISEV Consortium; Théry, C.; Witwer, K. W. Minimal Information for Studies of Extracellular Vesicles (MISEV2023): From Basic to Advanced Approaches. *J. Extracell. Vesicles* **2024**, *13* (2), e12404. https://doi.org/10.1002/jev2.12404.
(10) Feix, A. S.; Tabaie, E. Z.; Singh, A. N.; Wittenberg, N. J.; Wilson, E. H.; Joachim, A. An In-Depth Exploration of the Multifaceted Roles of EVs in the Context of Pathogenic Single-Cell Microorganisms. *Microbiol. Mol. Biol. Rev.* **2024**, e00037-24. https://doi.org/10.1128/mmbr.00037-24.
(11) Coelho, C.; Brown, L.; Maryam, M.; Vij, R.; Smith, D. F. Q.; Burnet, M. C.; Kyle, J. E.; Heyman, H. M.; Ramirez, J.; Prados-Rosales, R.; Lauvau, G.; Nakayasu, E. S.; Brady, N. R.; Hamacher-Brady, A.; Coppens, I.; Casadevall, A. Listeria Monocytogenes Virulence Factors, Including Listeriolysin O, Are Secreted in Biologically Active Extracellular Vesicles. *J. Biol. Chem.* **2019**, *294* (4), 1202–1217. https://doi.org/10.1074/jbc.RA118.006472.

View Article Online
DOI: 10.1039/D5NR05126F

(12) Singh, A. N.; Nice, J. B.; Wu, M.; Brown, A. C.; Wittenberg, N. J. Multivariate Analysis of Individual Bacterial Outer Membrane Vesicles Using Fluorescence Microscopy. *Chem. Biomed. Imaging* **2024**, cbmi.4c00014. https://doi.org/10.1021/cbmi.4c00014.

(13) Rivera, J.; Cordero, R. J. B.; Nakouzi, A. S.; Frases, S.; Nicola, A.; Casadevall, A. *Bacillus Anthracis* Produces Membrane-Derived Vesicles Containing Biologically Active Toxins. *Proc. Natl. Acad. Sci.* **2010**, *107* (44), 19002–19007. https://doi.org/10.1073/pnas.1008843107.

(14) Pérez-Cruz, C.; Delgado, L.; López-Iglesias, C.; Mercade, E. Outer-Inner Membrane Vesicles Naturally Secreted by Gram-Negative Pathogenic Bacteria. *PLOS ONE* **2015**, *10* (1), e0116896. https://doi.org/10.1371/journal.pone.0116896.

(15) Pérez-Cruz, C.; Carrión, O.; Delgado, L.; Martinez, G.; López-Iglesias, C.; Mercade, E. New Type of Outer Membrane Vesicle Produced by the Gram-Negative Bacterium Shewanella Vesiculosa M7 ^{T}: Implications for DNA Content. *Appl. Environ. Microbiol.* **2013**, *79* (6), 1874–1881. https://doi.org/10.1128/AEM.03657-12.

(16) Toyofuku, M.; Nomura, N.; Eberl, L. Types and Origins of Bacterial Membrane Vesicles. *Nat. Rev. Microbiol.* **2019**, *17* (1), 13–24. https://doi.org/10.1038/s41579-018-0112-2.

(17) Jeong, D.; Kim, M. J.; Park, Y.; Chung, J.; Kweon, H.-S.; Kang, N.-G.; Hwang, S. J.; Youn, S. H.; Hwang, B. K.; Kim, D. Visualizing Extracellular Vesicle Biogenesis in Gram-Positive Bacteria Using Super-Resolution Microscopy. *BMC Biol.* **2022**, *20* (1), 270. https://doi.org/10.1186/s12915-022-01472-3.

(18) Zhu, Y.; Zhao, J.; Ding, H.; Qiu, M.; Xue, L.; Ge, D.; Wen, G.; Ren, H.; Li, P.; Wang, J. Applications of Plant-derived Extracellular Vesicles in Medicine. *MedComm* **2024**, *5* (10), e741. https://doi.org/10.1002/mco2.741.

(19) Li, J.; Wang, Z.; Wang, F.; Du, X.; Pang, X. Plant-Derived Vesicles: Isolation Strategies and Therapeutic Applications. *Front. Plant Sci.* **2026**, *16*, 1660579. https://doi.org/10.3389/fpls.2025.1660579.

(20) Jo, H. Y.; Kang, S. J.; Kim, G.; Gwak, S.; Baek, G.; Rhee, W. J. Plant-derived Extracellular Vesicles: Current Status and Challenges for Developing a New Paradigm in Therapeutics Development. *VIEW* **2025**, *6* (1), 20240115. https://doi.org/10.1002/VIW.20240115.

(21) Kang, S. J.; Rhee, W. J. Engineered Plant-Derived Extracellular Vesicles as Targeted Drug Carriers in Cancer Therapy. *ACS Appl. Bio Mater.* **2026**, *9* (2), 1053–1063. https://doi.org/10.1021/acsabm.5c01943.

(22) Corvigno, S.; Liu, Y.; Bayraktar, E.; Stur, E.; Bayram, N. N.; Ahumada, A. L.; Nagaraju, S.; Rodriguez-Aguayo, C.; Chen, H.; Vu, T. C.; Wen, Y.; Liang, H.; Zhao, L.; Lee, S.; Lopez-Berestein, G.; Sood, A. K. Enhanced Plant-Derived Vesicles for Nucleotide Delivery for Cancer Therapy. *Npj Precis. Oncol.* **2024**, *8* (1), 86. https://doi.org/10.1038/s41698-024-00556-3.

(23) Joly, L.-M.; Tertel, T.; Sowislok, A.; Giebel, B.; Jäger, M. A New Subpopulation of Extracellular Vesicles Harvested from Osteogenically Induced Mesenchymal Stromal Cells of Surgical Site-Released Tissue. *Biomolecules* **2026**, *16* (2), 289. https://doi.org/10.3390/biom16020289.

(24) Nederveen, J. P.; Warnier, G.; Di Carlo, A.; Nilsson, M. I.; Tarnopolsky, M. A. Extracellular Vesicles and Exosomes: Insights From Exercise Science. *Front. Physiol.* **2021**, *11*, 604274. https://doi.org/10.3389/fphys.2020.604274.

(25) Silvestri, M.; Fantini, C.; Duranti, G.; Grazioli, E.; Caporossi, D.; Balbi, C.; Dimauro, I. Exercise-Derived Extracellular Vesicles in Oncology: A New Frontier for Translational Nanomedicine. *J. Transl. Med.* **2026**, *24* (1), 283. https://doi.org/10.1186/s12967-026-07742-w.

View Article Online
DOI: 10.1039/D5NR05126F

(26) Ciferri, M. C.; Quarto, R.; Tasso, R. Extracellular Vesicles as Biomarkers and Therapeutic Tools: From Pre-Clinical to Clinical Applications. *Biology* **2021**, *10* (5), 359. https://doi.org/10.3390/biology10050359.

(27) Kumar, M. A.; Baba, S. K.; Sadida, H. Q.; Marzooqi, S. Al.; Jerobin, J.; Altemani, F. H.; Algehainy, N.; Alanazi, M. A.; Abou-Samra, A.-B.; Kumar, R.; Al-Shabeeb Akil, A. S.; Macha, M. A.; Mir, R.; Bhat, A. A. Extracellular Vesicles as Tools and Targets in Therapy for Diseases. *Signal Transduct. Target. Ther.* **2024**, *9* (1), 27. https://doi.org/10.1038/s41392-024-01735-1.

(28) Yin, L.; Liu, X.; Shi, Y.; Ocansey, D. K. W.; Hu, Y.; Li, X.; Zhang, C.; Xu, W.; Qian, H. Therapeutic Advances of Stem Cell-Derived Extracellular Vesicles in Regenerative Medicine. *Cells* **2020**, *9* (3), 707. https://doi.org/10.3390/cells9030707.

(29) Karnas, E.; Dudek, P.; Zuba-Surma, E. K. Stem Cell- Derived Extracellular Vesicles as New Tools in Regenerative Medicine - Immunomodulatory Role and Future Perspectives. *Front. Immunol.* **2023**, *14*, 1120175. https://doi.org/10.3389/fimmu.2023.1120175.

(30) Ghosh, S.; Ghosh, S. Exosome: The “Off-the-Shelf” Cellular Nanocomponent as a Potential Pathogenic Agent, a Disease Biomarker, and Neurotherapeutics. *Front. Pharmacol.* **2022**, *13*, 878058. https://doi.org/10.3389/fphar.2022.878058.

(31) Si, Q.; Wu, L.; Pang, D.; Jiang, P. Exosomes in Brain Diseases: Pathogenesis and Therapeutic Targets. *MedComm* **2023**, *4* (3), e287. https://doi.org/10.1002/mco2.287.

(32) Kashyap, D.; Panda, M.; Baral, B.; Varshney, N.; R, S.; Bhandari, V.; Parmar, H. S.; Prasad, A.; Jha, H. C. Outer Membrane Vesicles: An Emerging Vaccine Platform. *Vaccines* **2022**, *10* (10), 1578. https://doi.org/10.3390/vaccines10101578.

(33) Wang, S.; Gao, J.; Wang, Z. Outer Membrane Vesicles for Vaccination and Targeted Drug Delivery. *WIREs Nanomedicine Nanobiotechnology* **2019**, *11* (2). https://doi.org/10.1002/wnan.1523.

(34) Micoli, F.; MacLennan, C. A. Outer Membrane Vesicle Vaccines. *Semin. Immunol.* **2020**, *50*, 101433. https://doi.org/10.1016/j.smim.2020.101433.

(35) Almeria, C.; Kreß, S.; Weber, V.; Egger, D.; Kasper, C. Heterogeneity of Mesenchymal Stem Cell-Derived Extracellular Vesicles Is Highly Impacted by the Tissue/Cell Source and Culture Conditions. *Cell Biosci.* **2022**, *12* (1), 51. https://doi.org/10.1186/s13578-022-00786-7.

(36) Allelein, S.; Medina-Perez, P.; Lopes, A. L. H.; Rau, S.; Hause, G.; Kölsch, A.; Kuhlmeier, D. Potential and Challenges of Specifically Isolating Extracellular Vesicles from Heterogeneous Populations. *Sci. Rep.* **2021**, *11* (1), 11585. https://doi.org/10.1038/s41598-021-91129-y.

(37) Roy, S.; Lin, H.-Y.; Chou, C.-Y.; Huang, C.-H.; Small, J.; Sadik, N.; Ayinon, C. M.; Lansbury, E.; Cruz, L.; Yekula, A.; Jones, P. S.; Balaj, L.; Carter, B. S. Navigating the Landscape of Tumor Extracellular Vesicle Heterogeneity. *Int. J. Mol. Sci.* **2019**, *20* (6), 1349. https://doi.org/10.3390/ijms20061349.

(38) Turner, L.; Bitto, N. J.; Steer, D. L.; Lo, C.; D’Costa, K.; Ramm, G.; Shambrook, M.; Hill, A. F.; Ferrero, R. L.; Kaparakis-Liaskos, M. Helicobacter Pylori Outer Membrane Vesicle Size Determines Their Mechanisms of Host Cell Entry and Protein Content. *Front. Immunol.* **2018**, *9*, 1466. https://doi.org/10.3389/fimmu.2018.01466.

(39) Mata, C.; Jeanne, O.; Jalali, M.; Lu, Y.; Mahshid, S. Nanostructured-Based Optical Readouts Interfaced with Machine Learning for Identification of Extracellular Vesicles (Adv. Healthcare Mater. 5/2023). *Adv. Healthc. Mater.* **2023**, *12*, 2370024. https://doi.org/10.1002/adhm.202370024.

(40) Imanbekova, M.; Suarasan, S.; Lu, Y.; Jurchuk, S.; Wachsmann-Hogiu, S. Recent Advances in Optical Label-Free Characterization of Extracellular Vesicles. *Nanophotonics* **2022**, *11* (12), 2827–2863. https://doi.org/10.1515/nanoph-2022-0057.

View Article Online
DOI: 10.1039/D5NR05126F

(41) Paolini, L.; Federici, S.; Consoli, G.; Arceri, D.; Radeghieri, A.; Alessandri, I.; Bergese, P. Fourier-transform Infrared (FT-IR) Spectroscopy Fingerprints Subpopulations of Extracellular Vesicles of Different Sizes and Cellular Origin. *J. Extracell. Vesicles* **2020**, *9* (1), 1741174. https://doi.org/10.1080/20013078.2020.1741174.
(42) Zini, J.; Saari, H.; Ciana, P.; Viitala, T.; Lõhmus, A.; Saarinen, J.; Yliperttula, M. Infrared and Raman Spectroscopy for Purity Assessment of Extracellular Vesicles. *Eur. J. Pharm. Sci.* **2022**, *172*, 106135. https://doi.org/10.1016/j.ejps.2022.106135.
(43) Liebel, M.; Hugall, J. T.; Van Hulst, N. F. Ultrasensitive Label-Free Nanosensing and High-Speed Tracking of Single Proteins. *Nano Lett.* **2017**, *17* (2), 1277–1281. https://doi.org/10.1021/acs.nanolett.6b05040.
(44) Wallucks, A.; DeCorwin-Martin, P.; Shen, M. L.; Ng, A.; Juncker, D. Size Photometry and Fluorescence Imaging of Immobilized Immersed Extracellular Vesicles.
(45) Taylor, R. W.; Sandoghdar, V. Interferometric Scattering Microscopy: Seeing Single Nanoparticles and Molecules via Rayleigh Scattering. *Nano Lett.* **2019**, *19* (8), 4827–4835. https://doi.org/10.1021/acs.nanolett.9b01822.
(46) Abbe, E. Beiträge Zur Theorie Des Mikroskops Und Der Mikroskopischen Wahrnehmung. *Arch. Für Mikrosk. Anat.* **1873**, *9* (1), 413–468. https://doi.org/10.1007/BF02956173.
(47) Van Der Pol, E.; Hoekstra, A. G.; Sturk, A.; Otto, C.; Van Leeuwen, T. G.; Nieuwland, R. Optical and Non-optical Methods for Detection and Characterization of Microparticles and Exosomes. *J. Thromb. Haemost.* **2010**, *8* (12), 2596–2607. https://doi.org/10.1111/j.1538-7836.2010.04074.x.
(48) Cavallaro, S.; Pevere, F.; Stridfeldt, F.; Görgens, A.; Paba, C.; Sahu, S. S.; Mamand, D. R.; Gupta, D.; El Andaloussi, S.; Linnros, J.; Dev, A. Multiparametric Profiling of Single Nanoscale Extracellular Vesicles by Combined Atomic Force and Fluorescence Microscopy: Correlation and Heterogeneity in Their Molecular and Biophysical Features. *Small* **2021**, *17* (14), 2008155. https://doi.org/10.1002/smll.202008155.
(49) Lee, K.; Fraser, K.; Ghaddar, B.; Yang, K.; Kim, E.; Balaj, L.; Chiocca, E. A.; Breakefield, X. O.; Lee, H.; Weissleder, R. Multiplexed Profiling of Single Extracellular Vesicles. *ACS Nano* **2018**, *12* (1), 494–503. https://doi.org/10.1021/acsnano.7b07060.
(50) Nikoloff, J. M.; Saucedo-Espinosa, M. A.; Dittrich, P. S. Microfluidic Platform for Profiling of Extracellular Vesicles from Single Breast Cancer Cells. *Anal. Chem.* **2023**, *95* (3), 1933–1939. https://doi.org/10.1021/acs.analchem.2c04106.
(51) Li, Z.; Guo, K.; Gao, Z.; Chen, J.; Ye, Z.; Cao, M.; Wang, S. E.; Yin, Y.; Zhong, W. Colocalization of Protein and microRNA Markers Reveals Unique Extracellular Vesicle Subpopulations for Early Cancer Detection. *Sci. Adv.* **2024**.
(52) Stears, R. L.; Martinsky, T.; Schena, M. Trends in Microarray Analysis. *Nat. Med.* **2003**, *9* (1), 140–145. https://doi.org/10.1038/nm0103-140.
(53) Jørgensen, M.; Bæk, R.; Pedersen, S.; Søndergaard, E. K. L.; Kristensen, S. R.; Varming, K. Extracellular Vesicle (EV) Array: Microarray Capturing of Exosomes and Other Extracellular Vesicles for Multiplexed Phenotyping. *J. Extracell. Vesicles* **2013**, *2* (1), 20920. https://doi.org/10.3402/jev.v2i0.20920.
(54) Martel, R.; Shen, M. L.; DeCorwin-Martin, P.; De Araujo, L. O. F.; Juncker, D. Extracellular Vesicle Antibody Microarray for Multiplexed Inner and Outer Protein Analysis. *ACS Sens.* **2022**, *7* (12), 3817–3828. https://doi.org/10.1021/acssensors.2c01750.
(55) Clegg, L.-A. M.; Sloth, J. K.; Bæk, R.; Jørgensen, M. M. Photometric Method for Dual Targeting of Surface and Surface-Associated Proteins on Extracellular Vesicles in the Multiparametric Test. *Front. Mol. Biosci.* **2022**, *9*, 917487. https://doi.org/10.3389/fmolb.2022.917487.
(56) Cawley, J. L.; Blauch, M. E.; Collins, S. M.; Nice, J. B.; Xie, Q.; Jordan, L. R.; Brown, A. C.; Wittenberg, N. J. Nanoarrays of Individual Liposomes and Bacterial Outer Membrane

View Article Online
DOI: 10.1039/D5NR05126F

Vesicles by Liftoff Nanocontact Printing. *Small* **2021**, *17* (50), 2103338. https://doi.org/10.1002/smll.202103338.
(57) Ricoult, S. G.; Pla-Roca, M.; Safavieh, R.; Lopez-Ayon, G. M.; Grütter, P.; Kennedy, T. E.; Juncker, D. Large Dynamic Range Digital Nanodot Gradients of Biomolecules Made by Low-Cost Nanocontact Printing for Cell Haptotaxis. *Small* **2013**, *9* (19), 3308–3313. https://doi.org/10.1002/smll.201202915.
(58) Homola, J. Surface Plasmon Resonance Sensors for Detection of Chemical and Biological Species. *Chem. Rev.* **2008**, *108* (2), 462–493. https://doi.org/10.1021/cr068107d.
(59) Kretschmann, E.; Raether, H. Notizen: Radiative Decay of Non Radiative Surface Plasmons Excited by Light. *Z. Für Naturforschung A* **1968**, *23* (12), 2135–2136. https://doi.org/doi:10.1515/zna-1968-1247.
(60) Jackman, J. A.; Rahim Ferhan, A.; Cho, N.-J. Nanoplasmonic Sensors for Biointerfacial Science. *Chem Soc Rev* **2017**, *46* (12), 3615–3660. https://doi.org/10.1039/C6CS00494F.
(61) Phizicky, E. M.; Fields, S. Protein-Protein Interactions: Methods for Detection and Analysis. *Microbiol. Rev.* **1995**, *59* (1), 94–123. https://doi.org/10.1128/mr.59.1.94-123.1995.
(62) Yildizhan, Y.; Driessens, K.; Tsao, H. S. K.; Boiy, R.; Thomas, D.; Geukens, N.; Hendrix, A.; Lammertyn, J.; Spasic, D. Detection of Breast Cancer-Specific Extracellular Vesicles with Fiber-Optic SPR Biosensor. *Int. J. Mol. Sci.* **2023**, *24* (4), 3764. https://doi.org/10.3390/ijms24043764.
(63) Wang, X.; Phan, M. M.; Sun, Y.; Koerber, J. T.; Ho, H.; Chen, Y.; Yang, J. Development of an SPR-Based Binding Assay for Characterization of Anti-CD20 Antibodies to CD20 Expressed on Extracellular Vesicles. *Anal. Biochem.* **2022**, *646*, 114635. https://doi.org/10.1016/j.ab.2022.114635.
(64) Kim, J.-Y.; Doody, A. M.; Chen, D. J.; Cremona, G. H.; Shuler, M. L.; Putnam, D.; DeLisa, M. P. Engineered Bacterial Outer Membrane Vesicles with Enhanced Functionality. *J. Mol. Biol.* **2008**, *380* (1), 51–66. https://doi.org/10.1016/j.jmb.2008.03.076.
(65) Chin, L. K.; Son, T.; Hong, J.-S.; Liu, A.-Q.; Skog, J.; Castro, C. M.; Weissleder, R.; Lee, H.; Im, H. Plasmonic Sensors for Extracellular Vesicle Analysis: From Scientific Development to Translational Research. *ACS Nano* **2020**, *14* (11), 14528–14548. https://doi.org/10.1021/acsnano.0c07581.
(66) Hsu, C.-C.; Yang, Y.; Kannisto, E.; Zeng, X.; Yu, G.; Patnaik, S. K.; Dy, G. K.; Reid, M. E.; Gan, Q.; Wu, Y. Simultaneous Detection of Tumor Derived Exosomal Protein–MicroRNA Pairs with an Exo-PROS Biosensor for Cancer Diagnosis. *ACS Nano* **2023**, *17* (9), 8108–8122. https://doi.org/10.1021/acsnano.2c10970.
(67) Yang, Y.; Zhai, C.; Zeng, Q.; Khan, A. L.; Yu, H. Multifunctional Detection of Extracellular Vesicles with Surface Plasmon Resonance Microscopy. *Anal. Chem.* **2020**, *92* (7), 4884–4890. https://doi.org/10.1021/acs.analchem.9b04622.
(68) Im, H.; Shao, H.; Park, Y. I.; Peterson, V. M.; Castro, C. M.; Weissleder, R.; Lee, H. Label-Free Detection and Molecular Profiling of Exosomes with a Nano-Plasmonic Sensor. *Nat. Biotechnol.* **2014**, *32* (5), 490–495. https://doi.org/10.1038/nbt.2886.
(69) Park, J.; Im, H.; Hong, S.; Castro, C. M.; Weissleder, R.; Lee, H. Analyses of Intravesicular Exosomal Proteins Using a Nano-Plasmonic System. *ACS Photonics* **2018**, *5* (2), 487–494. https://doi.org/10.1021/acsphotonics.7b00992.
(70) Jones, A. R. Light Scattering for Particle Characterization. *Prog. Energy Combust. Sci.* **1999**, *25* (1), 1–53. https://doi.org/10.1016/S0360-1285(98)00017-3.
(71) *Encyclopedia of Color Science and Technology*; Luo, M. R., Ed.; Springer New York: New York, NY, 2016. https://doi.org/10.1007/978-1-4419-8071-7.
(72) Miles, R. B.; Lempert, W. R.; Forkey, J. N. Laser Rayleigh Scattering. *Meas. Sci. Technol.* **2001**, *12* (5), R33–R51. https://doi.org/10.1088/0957-0233/12/5/201.

View Article Online
DOI: 10.1039/D5NR05126F

(73) Singh, A. N.; Nice, J. B.; Wu, M.; Brown, A. C.; Wittenberg, N. J. Multivariate Analysis of Individual Bacterial Outer Membrane Vesicles Using Fluorescence Microscopy. *Chem. Biomed. Imaging* **2024**, *2* (5), 352–361. https://doi.org/10.1021/cbmi.4c00014.

(74) Khan, M. A.; Anand, S.; Deshmukh, S. K.; Singh, S.; Singh, A. P. Determining the Size Distribution and Integrity of Extracellular Vesicles by Dynamic Light Scattering. In *Cancer Biomarkers*; Deep, G., Ed.; Methods in Molecular Biology; Springer US: New York, NY, 2022; Vol. 2413, pp 165–175. https://doi.org/10.1007/978-1-0716-1896-7_17.

(75) Sarra, A.; Celluzzi, A.; Bruno, S. P.; Ricci, C.; Sennato, S.; Ortore, M. G.; Casciardi, S.; Del Chierico, F.; Postorino, P.; Bordi, F.; Masotti, A. Biophysical Characterization of Membrane Phase Transition Profiles for the Discrimination of Outer Membrane Vesicles (OMVs) From Escherichia Coli Grown at Different Temperatures. *Front. Microbiol.* **2020**, *11*, 290. https://doi.org/10.3389/fmicb.2020.00290.

(76) Musante, L.; Bontha, S. V.; La Salvia, S.; Fernandez-Piñeros, A.; Lannigan, J.; Le, T. H.; Mas, V.; Erdbrügger, U. Rigorous Characterization of Urinary Extracellular Vesicles (uEVs) in the Low Centrifugation Pellet - a Neglected Source for uEVs. *Sci. Rep.* **2020**, *10* (1), 3701. https://doi.org/10.1038/s41598-020-60619-w.

(77) Holcar, M.; Ferdin, J.; Sitar, S.; Tušek-Žnidarič, M.; Dolžan, V.; Plemenitaš, A.; Žagar, E.; Lenassi, M. Enrichment of Plasma Extracellular Vesicles for Reliable Quantification of Their Size and Concentration for Biomarker Discovery. *Sci. Rep.* **2020**, *10* (1), 21346. https://doi.org/10.1038/s41598-020-78422-y.

(78) Lyu, T. S.; Ahn, Y.; Im, Y.-J.; Kim, S.-S.; Lee, K.-H.; Kim, J.; Choi, Y.; Lee, D.; Kang, E.; Jin, G.; Hwang, J.; Lee, S.; Cho, J.-A. The Characterization of Exosomes from Fibrosarcoma Cell and the Useful Usage of Dynamic Light Scattering (DLS) for Their Evaluation. *PLOS ONE* **2021**, *16* (1), e0231994. https://doi.org/10.1371/journal.pone.0231994.

(79) Bertolone, L.; Castagna, A.; Manfredi, M.; De Santis, D.; Ambrosani, F.; Antinori, E.; Mulatero, P.; Danese, E.; Marengo, E.; Barberis, E.; Veneri, M.; Martinelli, N.; Friso, S.; Pizzolo, F.; Olivieri, O. Proteomic Analysis of Urinary Extracellular Vesicles Highlights Specific Signatures for Patients with Primary Aldosteronism. *Front. Endocrinol.* **2023**, *14*, 1096441. https://doi.org/10.3389/fendo.2023.1096441.

(80) Carvalho, P. M.; Felício, M. R.; Santos, N. C.; Gonçalves, S.; Domingues, M. M. Application of Light Scattering Techniques to Nanoparticle Characterization and Development. *Front. Chem.* **2018**, *6*, 237. https://doi.org/10.3389/fchem.2018.00237.

(81) Bhattacharjee, S. DLS and Zeta Potential – What They Are and What They Are Not? *J. Controlled Release* **2016**, *235*, 337–351. https://doi.org/10.1016/j.jconrel.2016.06.017.

(82) Soo, C. Y.; Song, Y.; Zheng, Y.; Campbell, E. C.; Riches, A. C.; Gunn-Moore, F.; Powis, S. J. Nanoparticle Tracking Analysis Monitors Microvesicle and Exosome Secretion from Immune Cells. *Immunology* **2012**, *136* (2), 192–197. https://doi.org/10.1111/j.1365-2567.2012.03569.x.

(83) Sunkara, V.; Woo, H.-K.; Cho, Y.-K. Emerging Techniques in the Isolation and Characterization of Extracellular Vesicles and Their Roles in Cancer Diagnostics and Prognostics. *The Analyst* **2016**, *141* (2), 371–381. https://doi.org/10.1039/C5AN01775K.

(84) Stetefeld, J.; McKenna, S. A.; Patel, T. R. Dynamic Light Scattering: A Practical Guide and Applications in Biomedical Sciences. *Biophys. Rev.* **2016**, *8* (4), 409–427. https://doi.org/10.1007/s12551-016-0218-6.

(85) Božič, D.; Sitar, S.; Junkar, I.; Štukelj, R.; Pajnič, M.; Žagar, E.; Kralj-Iglič, V.; Kogej, K. Viscosity of Plasma as a Key Factor in Assessment of Extracellular Vesicles by Light Scattering. *Cells* **2019**, *8* (9), 1046. https://doi.org/10.3390/cells8091046.

(86) Kogej, K.; Božič, D.; Kobal, B.; Herzog, M.; Černe, K. Application of Dynamic and Static Light Scattering for Size and Shape Characterization of Small Extracellular Nanoparticles in

View Article Online
DOI: 10.1039/D5NR05126F

Plasma and Ascites of Ovarian Cancer Patients. *Int. J. Mol. Sci.* **2021**, *22* (23), 12946. https://doi.org/10.3390/ijms222312946.

(87) Wyatt, P. J. Multiangle Light Scattering: The Basic Tool for Macromolecular Characterization. *Instrum. Sci. Technol.* **1997**, *25* (1), 1–18. https://doi.org/10.1080/10739149709351443.

(88) Normak, K.; Papp, M.; Ullmann, M.; Paganini, C.; Manno, M.; Bongiovanni, A.; Bergese, P.; Arosio, P. Multiparametric Orthogonal Characterization of Extracellular Vesicles by Liquid Chromatography Combined with In-Line Light Scattering and Fluorescence Detection. *Anal. Chem.* **2023**, *95* (33), 12443–12451. https://doi.org/10.1021/acs.analchem.3c02108.

(89) Comfort, N.; Cai, K.; Bloomquist, T. R.; Strait, M. D.; Ferrante, A. W.; Baccarelli, A. A. Nanoparticle Tracking Analysis for the Quantification and Size Determination of Extracellular Vesicles. **2021**.

(90) McKinnon, K. M. Flow Cytometry: An Overview. *Curr. Protoc. Immunol.* **2018**, *120* (1). https://doi.org/10.1002/cpim.40.

(91) Doan, H.; Chinn, G. M.; Jahan-Tigh, R. R. Flow Cytometry II: Mass and Imaging Cytometry. *J. Invest. Dermatol.* **2015**, *135* (9), 1–4. https://doi.org/10.1038/jid.2015.263.

(92) Arkesteijn, G. J. A.; Lozano-Andrés, E.; Libregts, S. F. W. M.; Wauben, M. H. M. Improved Flow Cytometric Light Scatter Detection of Submicron-Sized Particles by Reduction of Optical Background Signals. *Cytometry A* **2020**, *97* (6), 610–619. https://doi.org/10.1002/cyto.a.24036.

(93) Morales-Kastresana, A.; Jones, J. C. Flow Cytometric Analysis of Extracellular Vesicles. In *Exosomes and Microvesicles*; Hill, A. F., Ed.; Methods in Molecular Biology; Springer New York: New York, NY, 2017; Vol. 1545, pp 215–225. https://doi.org/10.1007/978-1-4939-6728-5_16.

(94) De Rond, L.; Van Der Pol, E.; Hau, C. M.; Varga, Z.; Sturk, A.; Van Leeuwen, T. G.; Nieuwland, R.; Coumans, F. A. W. Comparison of Generic Fluorescent Markers for Detection of Extracellular Vesicles by Flow Cytometry. *Clin. Chem.* **2018**, *64* (4), 680–689. https://doi.org/10.1373/clinchem.2017.278978.

(95) Kuiper, M.; Van De Nes, A.; Nieuwland, R.; Varga, Z.; Van Der Pol, E. Reliable Measurements of Extracellular Vesicles by Clinical Flow Cytometry. *Am. J. Reprod. Immunol.* **2021**, *85* (2), e13350. https://doi.org/10.1111/aji.13350.

(96) Marchisio, M.; Simeone, P.; Bologna, G.; Ercolino, E.; Pierdomenico, L.; Pieragostino, D.; Ventrella, A.; Antonini, F.; Del Zotto, G.; Vergara, D.; Celia, C.; Di Marzio, L.; Del Boccio, P.; Fontana, A.; Bosco, D.; Miscia, S.; Lanuti, P. Flow Cytometry Analysis of Circulating Extracellular Vesicle Subtypes from Fresh Peripheral Blood Samples. *Int. J. Mol. Sci.* **2020**, *22* (1), 48. https://doi.org/10.3390/ijms22010048.

(97) Gao, X.; Teng, X.; Dai, Y.; Li, J. Rolling Circle Amplification-Assisted Flow Cytometry Approach for Simultaneous Profiling of Exosomal Surface Proteins. *ACS Sens.* **2021**, *6* (10), 3611–3620. https://doi.org/10.1021/acssensors.1c01163.

(98) Clayton, A.; Court, J.; Navabi, H.; Adams, M.; Mason, M. D.; Hobot, J. A.; Newman, G. R.; Jasani, B. Analysis of Antigen Presenting Cell Derived Exosomes, Based on Immuno-Magnetic Isolation and Flow Cytometry. *J. Immunol. Methods* **2001**, *247* (1–2), 163–174. https://doi.org/10.1016/S0022-1759(00)00321-5.

(99) Wieser, A.; Storz, E.; Liegl, G.; Peter, A.; Pritsch, M.; Shock, J.; Wai, S. N.; Schubert, S. Efficient Quantification and Characterization of Bacterial Outer Membrane Derived Nano-Particles with Flow Cytometric Analysis. *Int. J. Med. Microbiol.* **2014**, *304* (8), 1032–1037. https://doi.org/10.1016/j.ijmm.2014.07.012.

(100) Schetters, S. T. T.; Jong, W. S. P.; Horrevorts, S. K.; Kruijssen, L. J. W.; Engels, S.; Stolk, D.; Daleke-Schermerhorn, M. H.; Garcia-Vallejo, J.; Houben, D.; Unger, W. W. J.; Den Haan, J. M. M.; Luirink, J.; Van Kooyk, Y. Outer Membrane Vesicles Engineered to

View Article Online
DOI: 10.1039/D5NR05126F

Express Membrane-Bound Antigen Program Dendritic Cells for Cross-Presentation to CD8+ T Cells. *Acta Biomater.* **2019**, *91*, 248–257. https://doi.org/10.1016/j.actbio.2019.04.033.

(101) Sharma, M.; Sheth, M.; Poling, H. M.; Kuhnell, D.; Langevin, S. M.; Esfandiari, L. Rapid Purification and Multiparametric Characterization of Circulating Small Extracellular Vesicles Utilizing a Label-Free Lab-on-a-Chip Device. *Sci. Rep.* **2023**, *13* (1), 18293. https://doi.org/10.1038/s41598-023-45409-4.

(102) Von Lersner, A. K.; Fernandes, F.; Ozawa, P. M. M.; Jackson, M.; Masureel, M.; Ho, H.; Lima, S. M.; Vagner, T.; Sung, B. H.; Wehbe, M.; Franze, K.; Pua, H.; Wilson, J. T.; Irish, J. M.; Weaver, A. M.; Di Vizio, D.; Zijlstra, A. Multiparametric Single-Vesicle Flow Cytometry Resolves Extracellular Vesicle Heterogeneity and Reveals Selective Regulation of Biogenesis and Cargo Distribution. *ACS Nano* **2024**, *18* (15), 10464–10484. https://doi.org/10.1021/acsnano.3c11561.

(103) Prince, R. C.; Frontiera, R. R.; Potma, E. O. Stimulated Raman Scattering: From Bulk to Nano. *Chem. Rev.* **2017**, *117* (7), 5070–5094. https://doi.org/10.1021/acs.chemrev.6b00545.

(104) Tahir, M. A.; Dina, N. E.; Cheng, H.; Valev, V. K.; Zhang, L. Surface-Enhanced Raman Spectroscopy for Bioanalysis and Diagnosis. *Nanoscale* **2021**, *13* (27), 11593–11634. https://doi.org/10.1039/D1NR00708D.

(105) Le Ru, E. C.; Auguié, B. Enhancement Factors: A Central Concept during 50 Years of Surface-Enhanced Raman Spectroscopy. *ACS Nano* **2024**, *18* (14), 9773–9783. https://doi.org/10.1021/acsnano.4c01474.

(106) Ding, S.-Y.; You, E.-M.; Tian, Z.-Q.; Moskovits, M. Electromagnetic Theories of Surface-Enhanced Raman Spectroscopy. *Chem Soc Rev* **2017**, *46* (13), 4042–4076. https://doi.org/10.1039/C7CS00238F.

(107) Chaudhry, I.; Hu, G.; Ye, H.; Jensen, L. Toward Modeling the Complexity of the Chemical Mechanism in SERS. *ACS Nano* **2024**, *18* (32), 20835–20850. https://doi.org/10.1021/acsnano.4c07198.

(108) Lin, W.; Yuan, L.; Gao, Z.; Cai, G.; Liang, C.; Fan, M.; Xiu, X.; Huang, Z.; Feng, S.; Wang, J. An Integrated Sample-to-Answer SERS Platform for Multiplex Phenotyping of Extracellular Vesicles. *Sens. Actuators B Chem.* **2023**, *394*, 134355. https://doi.org/10.1016/j.snb.2023.134355.

(109) Diao, X.; Li, X.; Hou, S.; Li, H.; Qi, G.; Jin, Y. Machine Learning-Based Label-Free SERS Profiling of Exosomes for Accurate Fuzzy Diagnosis of Cancer and Dynamic Monitoring of Drug Therapeutic Processes. *Anal. Chem.* **2023**, *95* (19), 7552–7559. https://doi.org/10.1021/acs.analchem.3c00026.

(110) Liu, H.; Li, S.; Wang, J.; Su, J. Artificial Intelligence Virtual Extracellular Vesicles (AIVEVs). *Bioact. Mater.* **2026**, *61*, 34–55. https://doi.org/10.1016/j.bioactmat.2025.12.050.

(111) Kim, J.; Yang, J. D.; Agopian, V. G.; Zhu, Y.; Tseng, H.-R.; You, S. Computational Frameworks for Enhanced Extracellular Vesicle Biomarker Discovery. *Exp. Mol. Med.* **2026**, *58* (1), 73–81. https://doi.org/10.1038/s12276-025-01622-x.

(112) Greenberg, Z. F.; Graim, K. S.; He, M. Towards Artificial Intelligence-Enabled Extracellular Vesicle Precision Drug Delivery. *Adv. Drug Deliv. Rev.* **2023**, *199*, 114974. https://doi.org/10.1016/j.addr.2023.114974.

View Article Online
DOI: 10.1039/D5NR05126F

Data Availability Statement

No primary research results, software or code have been included and no new data were generated or analyzed as part of this review.